Matrix-valued Symmetric Templates for Interpolatory Surface Subdivisions, I: Regular Vertices

Charles K. Chui[*] Qingtang Jiang[†]

Department of Mathematics & Computer Science
University of Missouri–St. Louis
St. Louis, MO 63121

Abstract

The objective of this paper is to introduce a general procedure for deriving interpolatory surface subdivision schemes with "symmetric subdivision templates" (SSTs) for regular vertices. While the precise definition of "symmetry" will be clarified in the paper, the property of SSTs is instrumental to facilitate application of the standard procedure for finding symmetric weights for taking weighted averages to accommodate extraordinary (or irregular) vertices in surface subdivisions, a topic to be studied in a continuation paper. By allowing the use of matrices as weights, the SSTs introduced in this paper may be constructed to overcome the size barrier limited to scalar-valued interpolatory subdivision templates, and thus avoiding the unnecessary surface oscillation artifacts. On the other hand, while the old vertices in a (scalar) interpolatory subdivision scheme do not require a subdivision template, we will see that this is not the case for the matrix-valued setting. Here, we employ the same definition of interpolation subdivisions as in the usual scalar consideration, simply by requiring the old vertices to be stationary in the definition of matrix-valued interpolatory subdivisions. Hence, there would be another complication when the templates are extended to accommodate extraordinary vertices if the template sizes are not small. In this paper, we show that even for C^2 interpolatory subdivisions, only one "ring" is sufficient in general, for both old and new vertices. For example, for 1-to-4 split C^2 interpolatory surface subdivisions, we obtain matrix-valued symmetric interpolatory subdivision templates (SISTs) for both triangular and quadrilateral meshes with sizes that agree with those of the Loop and Catmull-Clark schemes, respectively. Matrix-valued SISTs of similar sizes are also constructed for C^2 interpolatory $\sqrt{3}$ and $\sqrt{2}$ subdivision schemes in this paper. In addition to small template sizes, an obvious feature of matrix-valued weights is the flexibility for introducing shape-control parameters. Another significance is that, in contrast to the usual scalar setting, matrix-valued SISTs can be formulated in terms of the coefficient sequence of some vector refinement equation of interpolating bivariate C^2 splines with small support. For example, by modifying the spline function vectors introduced in our previous work [3, 6], C^2 symmetric interpolatory subdivision schemes associated with refinement equations of C^2 cubic and quartic splines on the 6-directional and 4-directional meshes, respectively, are also constructed in this paper.

[*]Research supported by NSF Grant #CCR-0098331 and ARO Grant #W911NF-04-1-0298. This author is also with the Department of Statistics, Stanford University, Stanford, CA 94305.

[†]Research partially supported by a University of Missouri–St.Louis Research Award.

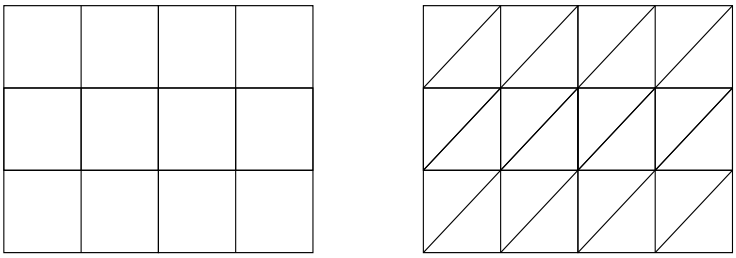

Figure 1: Two-directional and three-directional meshes

1. Introduction

Subdivision schemes provide an effective approach for efficient design and rendering of surfaces in the three-dimensional space (3-D). Formulated in terms of certain templates (also called coefficient stencils) of numerical values that are used as weights for taking weighted averages of certain given "old" vertices (or more precisely, points in 3-D) to generate "new" vertices, and perhaps to move the positions of the old vertices as well, a subdivision scheme is thereby applied to yield a higher resolution of some discrete approximation of the target (subdivision) surface, for each application (to be called iteration) of the weighted averages. If the old vertices are not altered for each iteration, the subdivision scheme is called an interpolatory subdivision scheme. Otherwise, it is called an approximation subdivision scheme. Subdivision templates are displayed in the two-dimensional space (2-D), along with certain triangles or quadrilaterals of regular shapes, in the so-called "parametric domains" (see, for example, Fig. 6 and Fig. 7). For regular vertices (also called ordinary vertices), these triangles and quadrilaterals, therefore, lie on 3-directional and 2-directional meshes, since the valences of regular vertices are 6 and 4, respectively. We will use a square grid to represent the 2-directional mesh as shown on the left of Fig. 1, and the 3-directional mesh can be easily generated by adding all the diagonals of the squares with only positive slope, as shown on the right of Fig. 1. For the purpose of displaying subdivision templates, however, we will use, as commonly done, the traditional equilateral triangular grid instead (see, for example, Fig. 6).

In general, subdivision templates for regular vertices are derived from the refinement equation (also called two-scale relation) of some bivariate refinable function (also called scaling function), with a finite refinement sequence (also called two-scale coefficient sequence). The refinement sequence is therefore called the "subdivision mask" of the subdivision scheme. For example, in the refinement equation:

$$\phi(\mathbf{x}) = \sum_{\mathbf{k}\in\mathbf{Z}^2} p_{\mathbf{k}}\phi(A\mathbf{x}-\mathbf{k}), \quad \mathbf{x}\in\mathbb{R}^2, \tag{1.1}$$

the function ϕ is a refinable function with (finite) subdivision mask $\{p_{\mathbf{k}}\}$ and dilation matrix A. We remark here that since the summation in the refinement equation is taken over the lattice $\mathbb{Z}^2$, it is natural and more effective to use the 2-directional and 3-directional meshes shown in Fig. 1 to represent the quadrilateral and triangular meshes,

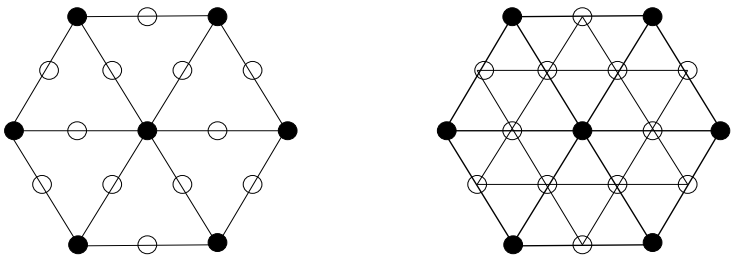

Figure 2: 1-to-4 split topological rule for triangular meshes

in the parametric domain, when the discussion is on the construction, rather than display, of subdivision masks.

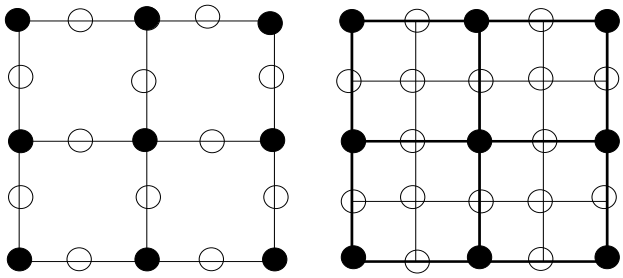

Figure 3: 1-to-4 split topological rule for quadrilateral meshes

It is clear that the subdivision mask sums to $|\det(A)|$ and that selection of the dilation matrix A necessarily depends on the connectivity rule, which is commonly called "topological rule" in the literature. The most commonly used topological rule is the "1-to-4 split" (dyadic) rule, that dictates the split of each triangle or square in the parametric domain into four sub-triangles or sub-squares by connecting the mid-points of the appropriate edges (see Fig. 2 for triangles and Fig. 3 for squares). Observe that in Fig. 3, a "face point" is introduced when the mid-points of the opposite edges of a square are connected. The new vertices introduced in the parametric domain, including the face points for the quadrilateral mesh, correspond to new vertices in 3-D, when the templates are applied to take weighted averages. Most of the well-known surface subdivision schemes such as the Loop [25], Catmull-Clark [1], and butterfly [9] schemes engage the 1-to-4 split topological rule. For the 1-to-4 split rule, the dilation matrix for the corresponding refinement equation to be selected is simply $2I_2$, both for the triangular and quadrilateral meshes. Other topological rules of interest include the $\sqrt{3}$ [23, 24, 20, 27, 21] and the $\sqrt{2}$ (or 4-to-8) [31, 32, 12, 14] topological rules, with dilation matrices given, for example, by

$$A_1 = \begin{bmatrix} 2 & -1 \\ 1 & -2 \end{bmatrix}, \quad A_2 = \begin{bmatrix} 1 & 1 \\ 1 & -1 \end{bmatrix}, \tag{1.2}$$

respectively. We remark that these matrices are certainly not unique, and that while the 1-to-4 split rule applies to both triangular and quadrilateral meshes, the $\sqrt{3}$ rule applies

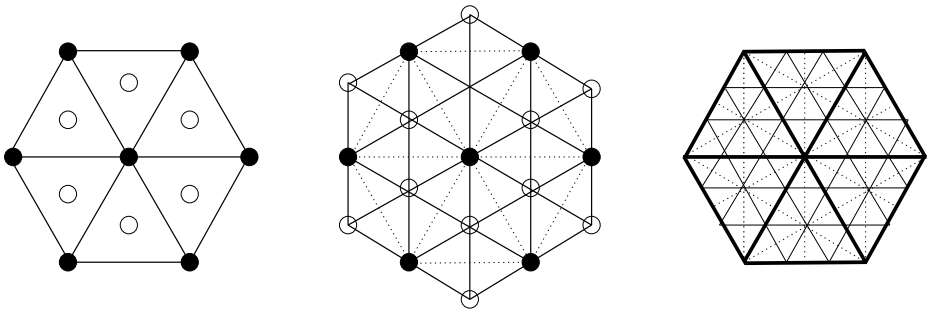

Figure 4: $\sqrt{3}$ topological rule

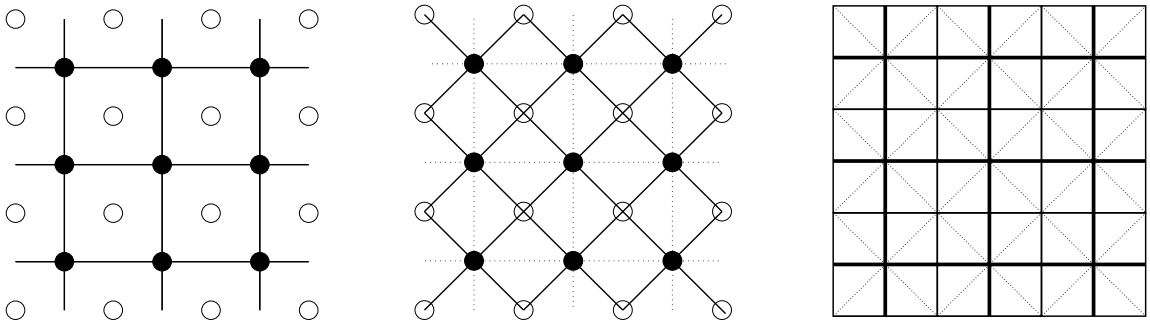

Figure 5: $\sqrt{2}$ (or 4-to-8) topological rule

only to the triangular mesh and the $\sqrt{2}$ rule to the quadrilateral mesh. See Fig. 4 and Fig. 5 for the $\sqrt{3}$ and $\sqrt{2}$ topological rules, respectively. The interested reader is referred to [15] for other topological rules.

To apply a subdivision scheme, the user must first select certain desirable points in 3-D as well as connect these points to form a triangular net or (non-planar) quadrilateral net. Hence, the points so chosen are vertices of the triangles or quadrilaterals. These points are called "control vertices", and the triangular or quadrilateral nets are called "control nets". For a control net with regular (or ordinary) control vertices $v_{\mathbf{k}}^0$, meaning that their valences are equal to 6 or 4, respectively, the refinement equation (1.1) immediately yields a "local averaging rule":

$$v_{\mathbf{k}}^{m+1} = \sum_{\mathbf{j}} v_{\mathbf{j}}^m p_{\mathbf{k}-A\mathbf{j}}, \quad m = 0, 1, \cdots, \tag{1.3}$$

where for each $m = 1, 2, \cdots$, $v_{\mathbf{k}}^m$ denote the set of newly generated points (vertices) in $\mathbb{R}^3$ obtained after applying the local averaging rule m times (or using the corresponding subdivision templates to perform m iterations). Since each iteration increases the resolution by (approximately) $|\det(A)|$ times, the vertices $v_{\mathbf{k}}^m$, for sufficiently large values of m, provide an accurate discrete approximation of the target subdivision surface, which is precisely given by the series representation

$$f(\mathbf{x}) = \sum_{\mathbf{k}} v_{\mathbf{k}}^0 \phi(\mathbf{x} - \mathbf{k}), \quad \mathbf{x} \in \mathbb{R}^2, \tag{1.4}$$

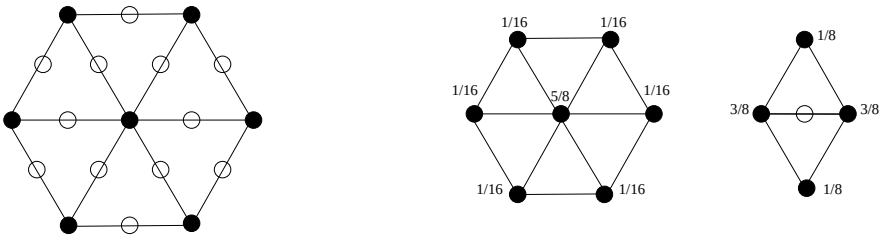

Figure 6: Subdivision templates of the Loop scheme for regular vertices (for moving the old vertices and generating a new vertex corresponding to an edge point, respectively)

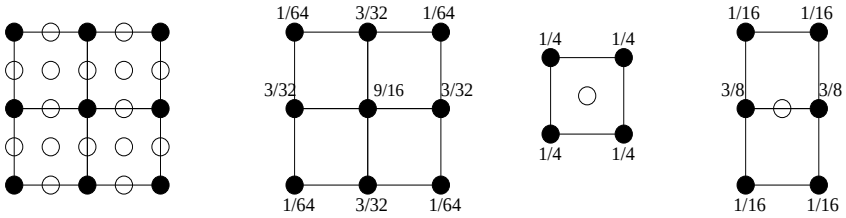

Figure 7: Subdivision templates of the Catmull-Clark scheme for regular vertices (for moving the old vertices, generating a new vertex corresponding to a face point, and generating a new vertex corresponding to an edge point, respectively)

with the control vertices $v^0_{\mathbf{k}}$ as coefficients. In other words, the subdivision scheme provides a very efficient way to render the surface $f(\mathbf{x})$ in (1.4), and the smoothness of this limiting (subdivision) surface is directed reflected by the smoothness of the refinable function $\phi(\mathbf{x})$.

The subdivision templates corresponding to the subdivision mask $\{p_{\mathbf{k}}\}$ can be easily formulated by applying (1.3). For example, for the dilation matrix $A = 2I_2$, with ϕ being the 3-directional box-spline B_{222}, we have the subdivision templates for the Loop scheme (for regular vertices) as shown in Fig. 6; and with ϕ being the tensor-product cardinal B-splines of order 4 (i.e. C^2 bi-cubic B-splines), we have the subdivision templates for the Catmull-Clark scheme (for regular vertices) as shown in Fig. 7.

For some applications, such as 3-D surface reversed engineering where data points are used as control vertices, interpolatory schemes are highly desirable. Unfortunately both the Loop and Catmull-Clark schemes are only approximation subdivision schemes as can

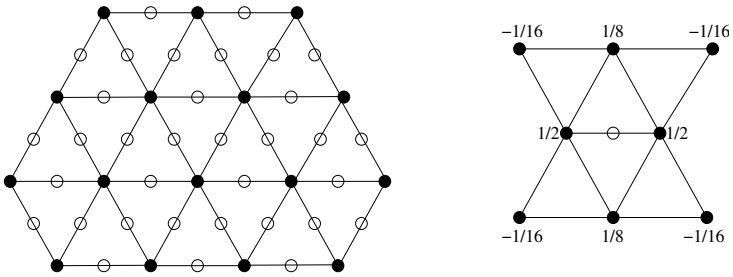

Figure 8: Subdivision template of the butterfly scheme (on right)

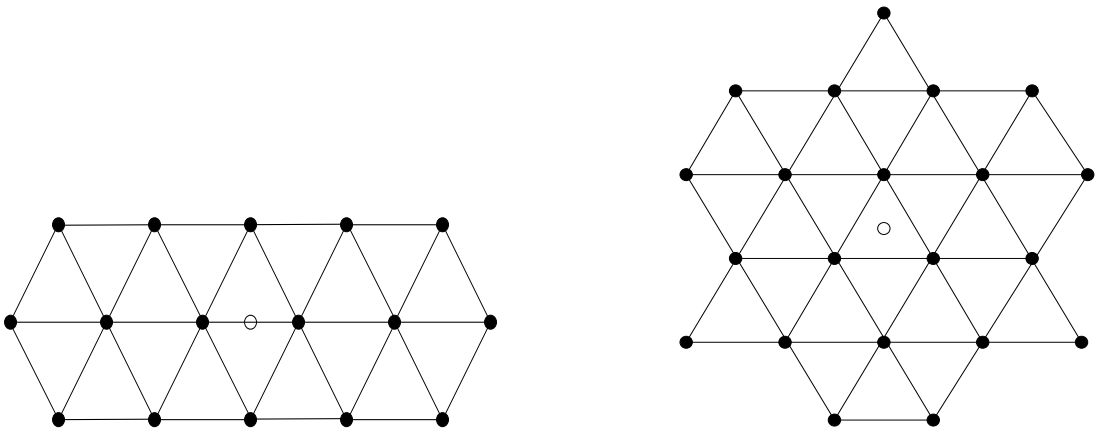

Figure 9: Template sizes of the C^2 1-to-4 split interpolatory scheme in [30] (on left) and the C^2 $\sqrt{3}$ interpolatory scheme [21] (on right)

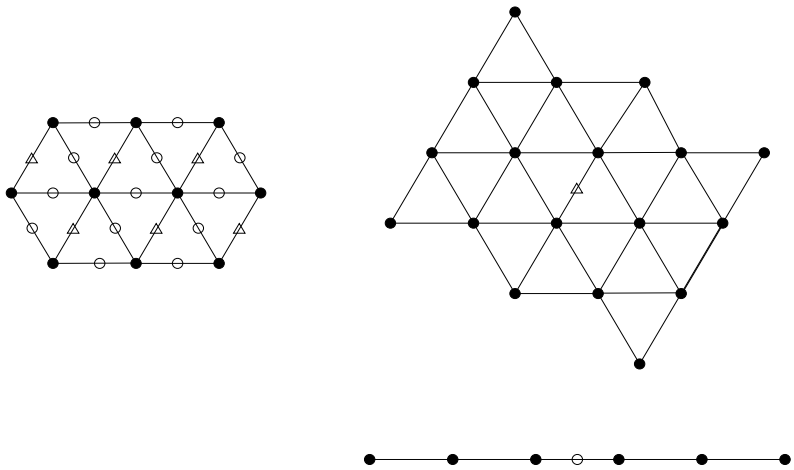

Figure 10: Two types of subdivision templates (on right) in [11] corresponding to two edge points in the parametric domain (on left) with different orientations

be seen from the first templates in Fig. 6 and Fig. 7. On the other hand, although the butterfly scheme (see Fig. 8) as well as certain more recent ones, such as those introduced in [24] and [22], are interpolatory, yet they only apply to generating C^1 subdivision surfaces even for regular control vertices (see [10, Cor.4.3]). Observe that in Fig. 8, there is only one template for generating a new vertex corresponding to an edge point. Since the old vertices are stationary, independent of the adjacent vertices, a template for the old vertices is not needed for the scalar-valued setting. The interpolating schemes in [24] are for $\sqrt{3}$-subdivision, and the one in [22] applies to the quadrilateral mesh in terms of the tensor-product of two copies of 1-D 4-point scheme. In general, taking the tensor-product of two 1-D C^2 interpolatory schemes gives a C^2 interpolatory surface subdivision scheme for regular vertices on a quadrilateral mesh, but the templates are necessarily undesirably large, thus yielding subdivision surfaces with undesirable oscillations. For the triangular 3-directional mesh, interpolatory schemes for higher orders of smoothness

introduced in [30] (for 1-to-4 split subdivision) and [21] (for $\sqrt{3}$ subdivision) also have large template sizes (see Fig. 9 for the template sizes of these two C^2 interpolatory schemes). Furthermore, interpolatory schemes corresponding to refinable functions with optimal smoothness order are given in [11]. However, the templates for the triangular mesh, which can be easily derived from [11], have large size (causing surface oscillation artifact) and depend on mesh orientations (creating serious difficulty to modify the templates in accommodating extraordinary vertices). See Fig. 10 for the template sizes for a C^2 interpolatory scheme in [11] and observe that to create new vertices in 3-D that correspond to the two different edge points in the parametric domain (shown in the figures by using "circles" and "triangles"), two different subdivision templates are used.

The objective of this paper is to present a general procedure for constructing interpolatory surface subdivision schemes with small symmetric subdivision templates (SSTs) by allowing matrices as weights. Here, the notion of symmetry requires not only the use of the same template for all old vertices and the same template for the new vertices of the same type (such as edge points or face points for the quadrilateral mesh), but also certain symmetric properties of the templates, regardless of orientations. To demonstrate our procedure, we will first use 2×2 and 3×3 matrices as weights to construct symmetric C^2 interpolatory 1-to-4 split subdivision schemes for both triangular and quadrilateral meshes, with template sizes identical with those of the Loop and Catmull-Clark schemes, respectively. We will also follow this procedure to construct symmetric C^2 interpolatory $\sqrt{3}$ and $\sqrt{2}$ subdivision schemes with analogously small template size. Furthermore, we will show that our procedure can be modified even for the construction of spline-based interpolatory surface subdivision schemes with SSTs, provided that certain suitable refinable vectors of bivariate spline functions exist. This would eliminate the need of adjusting free parameters to achieve smooth refinable function vectors. To demonstrate this, we apply the conditions for matrix-valued interpolatory subdivisions to modify the refinable spline function vectors constructed in [3, 6], resulting in two C^2 interpolatory schemes with SSTs and the corresponding refinable functions being C^2 cubics splines on the 6-directional mesh and C^2 quartic splines on the 4-directional mesh, respectively. In this regard, we point out that the interpolatory schemes in [9, 22, 30, 11, 12, 24, 20, 21] have nothing to do with spline refinement.

The procedure outlined in this paper can be applied to other topological rules such as $\sqrt{7}$ and $\sqrt{5}$ topological rules studied in [26] and [16], respectively. Furthermore, the extension of the smoothness-preservation results in [29, 28] for the extraordinary vertices from the scalar setting to the matrix-valued subdivisions are studied in our work [5].

This paper is organized as follows. In Section 2, the notion of control vectors, control vertices, and shape-control parameters for matrix-valued surface subdivisions is introduced, and a formulation of the (limiting) subdivision surfaces is given. In the first subsection, §2.1, a precise definition of matrix-valued interpolatory subdivision is defined (for the first time in the open literature, we believe), and equivalent formulations in terms of the corresponding subdivision masks and of the refinable function vectors, are derived in Propositions 1 and 2, respectively. In the second subsection, §2.2, the notion of "symmetric subdivision templates" (SSTs) is introduced, and equivalent sym-

metry properties of the corresponding subdivision masks are formulated in Theorems 1 and 2 for the topological rules discussed above. In addition, the properties of symmetry for the corresponding refinable function (or distribution) vectors are derived in Theorems 3 and 4. The main results of this paper are presented in Section 3 and the final section, Section 4. In the first subsection, §3.1, of Section 3, matrix-valued SSTs for C^2 interpolatory surface subdivision for the triangular mesh are constructed for the 1-to-4 split topological rule (in §3.1.1) and the $\sqrt{3}$ topological rule (in §3.1.2). Also, in the second subsection, §3.2, of Section 3, matrix-valued SSTs for C^2 interpolatory surface subdivision for the quadrilateral mesh are constructed for the 1-to-4 split topological rule (in §3.2.1) and the $\sqrt{2}$ topological rule (in §3.2.2). To facilitate the presentation of the construction of these SSTs, as well as to discuss the order of smoothness of the subdivision surfaces, a brief discussion is given in the beginning of Section 3. In the final section, matrix-valued symmetric interpolatory subdivision templates (SISTs) for designing and rendering interpolatory C^2 spline surfaces of degrees 3 and 4 are derived. These derivations are based on the refinable C^2 bivariate spline function vectors of degrees 3 and 4, on the 6-directional and 4-directional meshes, introduced in [3] and [6], respectively.

2. Interpolatory subdivisions with symmetric subdivision templates (SSTs)

For regular vertices, analogous to the current subdivision schemes with scalar-valued weights, as discussed in the previous section, a subdivision scheme with matrix-valued weights is derived from some vector-valued refinement equation

$$\Phi(\mathbf{x}) = \sum_{\mathbf{k}\in\mathbf{Z}^2} P_{\mathbf{k}}\Phi(A\mathbf{x}-\mathbf{k}), \quad \mathbf{x}\in\mathbb{R}^2, \tag{2.1}$$

but with matrix-valued subdivision mask $\{P_{\mathbf{k}}\}$ for a suitable dilation matrix A, where $\Phi = [\phi_0, \phi_1, \cdots, \phi_{r-1}]^T$ is called a refinable (or scaling) function vector. For the refinable function vector to be useful for surface subdivisions in our discussion, its components $\phi_\ell, \ell = 0, \cdots, r-1$, must be in C^2 and have compact support, and its subdivision mask must be finite and satisfy the condition of "generalized partition of unity":

$$\sum_{\mathbf{k}\in\mathbf{Z}^2} \mathbf{w}\Phi(x-\mathbf{k}) \equiv 1, \quad \mathbf{x}\in\mathbb{R}^2, \tag{2.2}$$

for some constant r-vector $\mathbf{w} = [w_0, w_1, \cdots, w_{r-1}]$. By changing the order of the ϕ_ℓs and multiplying them with some constant, if necessary, we may and will, assume that

$$w_0 = 1. \tag{2.3}$$

Corresponding to the refinement equation (2.1), the local averaging rule, from which the subdivision templates (with matrices as weights) follows immediately, is given by

$$\mathbf{v}_{\mathbf{k}}^{m+1} = \sum_{\mathbf{j}} \mathbf{v}_{\mathbf{j}}^m P_{\mathbf{k}-A\mathbf{j}}, \quad m = 0, 1, \cdots, \tag{2.4}$$

where

$$\mathbf{v}_{\mathbf{k}}^m =: [v_{\mathbf{k}}^m, s_{\mathbf{k},1}^m \cdots, s_{\mathbf{k},r-1}^m] \tag{2.5}$$

are "row-vectors" with r components of points $v_{\mathbf{k}}^m, s_{\mathbf{k},i}^m$, $i = 1, \cdots, r-1$, in $\mathbb{R}^3$. We will use the first components $v_{\mathbf{k}}^m$ as the vertices of the triangular or (non-planar) quadrilateral nets for the m-th iteration. Therefore, for sufficiently large values of m, the vertices $v_{\mathbf{k}}^m$ provide an accurate discrete approximation of the target subdivision surface. In [5], we have shown that this subdivision surface is precisely given by the series representation:

$$F(\mathbf{x}) = \sum_{\mathbf{k}} v_{\mathbf{k}}^0 \phi_0(\mathbf{x} - \mathbf{k}) + \sum_{\mathbf{k}} \Big(s_{\mathbf{k},1}^0 \phi_1(\mathbf{x} - \mathbf{k}) + \cdots + s_{\mathbf{k},r-1}^0 \phi_{r-1}(\mathbf{x} - \mathbf{k}) \Big). \tag{2.6}$$

with $[v_{\mathbf{k}}^0, s_{\mathbf{k},1}^0, \cdots, s_{\mathbf{k},r-1}^0]$ as coefficients, provided that the iteration process converges. Of course, the assumption (2.3) is essential for the first components to be used as vertices. We will call the initial row vectors $\mathbf{v}_{\mathbf{k}}^0$, "control vectors", their first components $v_{\mathbf{k}}^0$, "control vertices", and the other components $s_{\mathbf{k},1}^0, \cdots, s_{\mathbf{k},r-1}^0$, "shape-control parameters".

For a mask $\{P_{\mathbf{k}}\}$ with dilation matrix A, let

$$P(\omega) := \frac{1}{|\det A|} \sum_{\mathbf{k}} P_{\mathbf{k}} e^{-i\mathbf{k}\omega}, \ \omega = (\omega_1, \omega_2), \tag{2.7}$$

be the two-scale symbol of the mask $\{P_{\mathbf{k}}\}$. Then the refinement equation (2.1) can be re-formulated in the Fourier domain, as

$$\widehat{\Phi}(\omega) = P((A^{-1})^T \omega) \widehat{\Phi}((A^{-1})^T \omega). \tag{2.8}$$

In particular, we have $\widehat{\Phi}(0) = P(0)\widehat{\Phi}(0)$. In addition, since it follows from (2.2) that $\widehat{\Phi}(0) \neq [0, \cdots, 0]^T$, we see that $\widehat{\Phi}(0)$ is an eigenvector associated with the eigenvalue 1 of $P(0)$. In the following, we only consider subdivision masks for which 1 is a simple eigenvalue of $P(0)$ and other eigenvalues λ of $P(0)$ satisfy $|\lambda| < 1$. Under this additional assumption, it is well-known that the Fourier transform of Φ is given by

$$\begin{aligned} \widehat{\Phi}(\omega) &= P((A^{-1})^T \omega) P((A^{-2})^T \omega) \widehat{\Phi}((A^{-2})^T \omega) \\ &= P((A^{-1})^T \omega) P((A^{-2})^T \omega) \cdots \mathbf{u}_0 = \Pi_{n=1}^{\infty} P((A^{-n})^T \omega) \mathbf{u}_0, \end{aligned} \tag{2.9}$$

where $\mathbf{u}_0$, such as $\widehat{\Phi}(0)$ above, is an eigenvector associated with the eigenvalue 1 of $P(0)$.

2.1 Interpolatory subdivision schemes

As already discussed in the introduction section, a subdivision scheme is called interpolatory, if the positions of the vertices of the triangular or (non-planar) quadrilateral nets remain unchanged for each iteration of the subdivision process. In other words, the control vertices are stationary and lie on the limiting (subdivision) surface. We adopt this (geometric) requirement as the definition of interpolatory subdivision schemes, even when matrix-valued subdivision templates are applied. More precisely, in view of (2.3) and (2.4), we have the following.

Definition 1 *A matrix-valued subdivision scheme with matrix-valued mask* $\{P_{\mathbf{k}}\}$ *and dilation matrix* A *is said to be* **interpolatory***, if for any given control vectors* $\mathbf{v}_{\mathbf{k}}^0$*, the first components* $v_{A\mathbf{k}}^m$ *of* $\mathbf{v}_{A\mathbf{k}}^m$*,* $m = 1, 2, \cdots$*, in* (2.4) *are the same as the corresponding first components of the control vectors* $\mathbf{v}_{\mathbf{k}}^{m-1}$*; i.e.,*

$$v_{A\mathbf{k}}^m = v_{\mathbf{k}}^{m-1}, \quad m = 1, 2, \cdots. \tag{2.10}$$

We believe that this definition of interpolatory subdivisions is new for matrix-valued subdivision, though it is clearly a natural extension of that for the scalar-valued setting from $r = 1$ to the general r-dimensional matrices. We remark that in the vector-subdivision literature, there are other more restrictive definitions. For example, in [8] Hermite-type interpolation with other components of the refinable function vector to be specified as certain derivatives of the first component is considered, and the definition in [7] requires that other components of the refinable function vector to be interopolatory as well. These definitions are too restrictive for the discovery of a general class of matrix-valued interpolatory subdivision templates. On the other hand, Hermite interpolatory subdivision schemes are constructed in [13, 3, 4, 6], but the templates of these schemes do not satisfy the desirable symmetry property.

The algebraic property of an interpolatory mask $\{p_{\mathbf{k}}\}$ for the scalar-valued setting is given by

$$p_{A\mathbf{j}} = \delta(\mathbf{j}), \quad \mathbf{j} \in \mathbb{Z}^2, \tag{2.11}$$

where A is the dilation matrix in the refinement equation. In fact, this property is equivalent to the above definition of interpolatory subdivisions when the dimension r is reduced to 1. However, for the matrix-valued setting, the subdivision mask of an interpolatory subdivision scheme does not necessarily satisfy the condition:

$$P_{A\mathbf{j}} = \mathbf{0}, \quad \mathbf{j} \in \mathbb{Z}^2 \backslash \{(0,0)\}.$$

In the following, we derive a precise algebraic property of an interpolatory subdivision mask for the matrix-valued setting.

Proposition 1 *A subdivision scheme with matrix-valued mask* $\{P_{\mathbf{k}}\}$ *and dilation matrix* A *is interpolatory if and only if* $P_{A\mathbf{j}}$ *takes on the form:*

$$P_{0,0} = \begin{bmatrix} 1 & * & \cdots & * \\ 0 & * & \cdots & * \\ \vdots & \vdots & \cdots & \vdots \\ 0 & * & \cdots & * \end{bmatrix}, \quad P_{A\mathbf{j}} = \begin{bmatrix} 0 & * & \cdots & * \\ \vdots & \vdots & \cdots & \vdots \\ 0 & * & \cdots & * \end{bmatrix}, \quad \mathbf{j} \in \mathbb{Z}^2 \backslash \{(0,0)\}; \tag{2.12}$$

that is, the first column of $P_{0,0}$ *must be the unit vector* $[1, 0, \cdots, 0]^T$ *and the first columns of the other* $P_{A\mathbf{j}}$ *must be the zero vector, for* $\mathbf{j} \neq (0,0)$*.*

Proof. The proof is somewhat straightforward. Indeed, since we have

$$\mathbf{v}_{A\mathbf{k}}^{m+1} = \sum_{\mathbf{j}} \mathbf{v}_{\mathbf{j}}^m \; P_{A\mathbf{k}-A\mathbf{j}} = \sum_{\mathbf{j}} \mathbf{v}_{\mathbf{k}-\mathbf{j}}^m \; P_{A\mathbf{j}},$$

by (2.4), it follows that the first column of $\mathbf{v}_{A\mathbf{k}}^{m+1}$ is given by

$$\mathbf{v}_{A\mathbf{k}}^{m+1}[1,0,\cdots,0]^T = \mathbf{v}_{\mathbf{k}}^m P_{0,0}[1,0,\cdots,0]^T + \sum_{\mathbf{j}\neq(0,0)} \mathbf{v}_{\mathbf{k}-\mathbf{j}}^m P_{A\mathbf{j}}[1,0,\cdots,0]^T. \tag{2.13}$$

Therefore, for the scheme to be interpolatory, we have, by definition, $\mathbf{v}_{A\mathbf{k}}^{m+1}[1,0,\cdots,0]^T = \mathbf{v}_{\mathbf{k}}^m[1,0,\cdots,0]^T$, and this holds, if and only if the right-hand side of (2.13) is equal to $\mathbf{v}_{\mathbf{k}}^m[1,0,\cdots,0]^T$, which is the same as

$$P_{0,0}[1,0,\cdots,0]^T = [1,0,\cdots,0]^T, \quad P_{A\mathbf{j}}[1,0,\cdots,0]^T = [0,\cdots,0], \quad \mathbf{j}\neq(0,0);$$

that is, (2.12) holds. $\diamond$

Since we only consider finite subdivision masks, we will assume, without loss of generality, that $P_{\mathbf{k}} = 0, \mathbf{k} \notin [-N,N]^2$, for some $N \geq 1$. Let

$$\Omega := \{\sum_{k=1}^{\infty} A^{-k}\mathbf{x}_k : \quad \mathbf{x}_k \in [-N,N]^2,\ k \in \mathbb{N}\}. \tag{2.14}$$

Then it follows that $\operatorname{supp}\Phi := \cup_{\ell=0}^{r-1}\operatorname{supp}(\phi_\ell) \subset \Omega$ (see e.g., [19]). In the following, we use the notation $[\Omega] = \Omega \cap \mathbb{Z}^2$, and let $|[\Omega]|$ denote its cardinality. From the refinement equation (2.1), we have, for $\mathbf{j} \in [\Omega]$,

$$\Phi(\mathbf{j}) = \sum_{\mathbf{k}} P_{\mathbf{k}}\Phi(A\mathbf{j}-\mathbf{k}) = \sum_{\mathbf{k}} P_{A\mathbf{j}-\mathbf{k}}\Phi(\mathbf{k}) = \sum_{\mathbf{k}\in[\Omega]} P_{A\mathbf{j}-\mathbf{k}}\Phi(\mathbf{k}). \tag{2.15}$$

So, if we consider the column $r \times |[\Omega]|$-vector, $\operatorname{vec}(\Phi) := \Big[\Phi(\mathbf{j})\Big]_{\mathbf{j}\in[\Omega]}$, then it follows from (2.15) that

$$\operatorname{vec}(\Phi) = \Big[P_{A\mathbf{j}-\mathbf{k}}\Big]_{\mathbf{j},\mathbf{k}\in[\Omega]} \operatorname{vec}(\Phi).$$

In other words, $\operatorname{vec}(\Phi)$ is an eigenvector of $\Big[P_{A\mathbf{j}-\mathbf{k}}\Big]_{\mathbf{j},\mathbf{k}\in[\Omega]}$ associated with the eigenvalue 1. On the other hand, it is easy to verify that the $P_{\mathbf{k}}$s take on the form of (2.12), if and only if the column vector $\Big[\mathbf{L}_{\mathbf{j}}\Big]_{\mathbf{j}\in[\Omega]}$, where $\mathbf{L}_{\mathbf{j}} = \delta(\mathbf{j})[1,0,\cdots,0]^T$, is also an eigenvector of $\Big[P_{A\mathbf{j}-\mathbf{k}}\Big]_{\mathbf{j},\mathbf{k}\in[\Omega]}$ corresponding to the eigenvalue 1. Therefore, we have the following result, of which the 1-dimensional case was already considered in [33].

Proposition 2 *Let Φ be a refinable function vector with dilation matrix A and subdivision mask $\{P_{\mathbf{k}}\}$ that satisfies $P_{\mathbf{k}} = 0, \mathbf{k} \notin [-N,N]^2$. Also, let Φ be continuous and that 1 is a simple eigenvalue of the matrix $\Big[P_{A\mathbf{j}-\mathbf{k}}\Big]_{\mathbf{j},\mathbf{k}\in[\Omega]}$. Then the subdivision scheme associated with $\{P_{\mathbf{k}}\}$ is interpolatory if and only if Φ satisfies:*

$$\Phi(\mathbf{j}) = \delta(\mathbf{j})[1,0,\cdots,0]^T, \quad \mathbf{j} \in \mathbb{Z}^2. \tag{2.16}$$

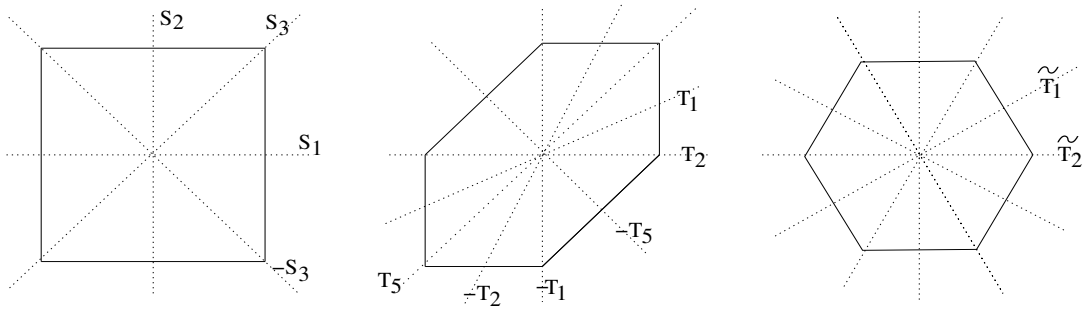

Figure 11: Symmetry "directions" or lines of symmetric reflection (shown in dotted lines on left and on right)

2.2 Symmetric masks and SSTs

In this subsection, we introduce the notion of symmetric subdivision templates (SSTs) and remark that this definition does not restrict to interpolatory subdivisions. Our goal is to show that the subdivision templates of a matrix-valued subdivision scheme are SSTs, if and only if the corresponding mask $\{P_{\mathbf{k}}\}$ satisfies the following symmetry conditions:

(i) For the quadrilateral mesh,

$$P_{\mathbf{k}} = P_{S_1\mathbf{k}} = P_{S_2\mathbf{k}} = P_{S_3\mathbf{k}}, \quad \mathbf{k} \in \mathbb{Z}^2, \tag{2.17}$$

where

$$S_1 = \begin{bmatrix} 1 & 0 \\ 0 & -1 \end{bmatrix}, \quad S_2 = \begin{bmatrix} -1 & 0 \\ 0 & 1 \end{bmatrix}, \quad S_3 = \begin{bmatrix} 0 & 1 \\ 1 & 0 \end{bmatrix}.$$

(ii) For the triangular mesh,

$$P_{\mathbf{k}} = P_{T_1\mathbf{k}} = P_{T_2\mathbf{k}}, \quad \mathbf{k} \in \mathbb{Z}^2, \tag{2.18}$$

where

$$T_1 = \begin{bmatrix} 1 & 0 \\ 1 & -1 \end{bmatrix}, \quad T_2 = \begin{bmatrix} 1 & -1 \\ 0 & -1 \end{bmatrix}.$$

Note that $S_1S_2S_3 = -S_3$. Thus, if the $P_{\mathbf{k}}$s satisfy (2.17), then $P_{-S_3\mathbf{k}} = P_{\mathbf{k}}$, and hence they satisfy the four-directional symmetry property (with lines of symmetric reflection shown on the left of Fig. 11, where the transformation matrices are also provided).

Note also that the two matrices T_1 and T_2 generate

$$T_3 := T_1T_2 = \begin{bmatrix} 1 & -1 \\ 1 & 0 \end{bmatrix}, \quad T_4 := T_2T_1 = \begin{bmatrix} 0 & 1 \\ -1 & 1 \end{bmatrix},$$
$$T_5 := T_1T_2T_1 = S_3, \qquad (T_1T_2)^3 = -I_2.$$

Therefore, if the $P_{\mathbf{k}}$s satisfy (2.18), then they satisfy the six-directional symmetry property (with lines of symmetric reflection shown in the middle of Fig. 11, where the transformation matrices are also provided).

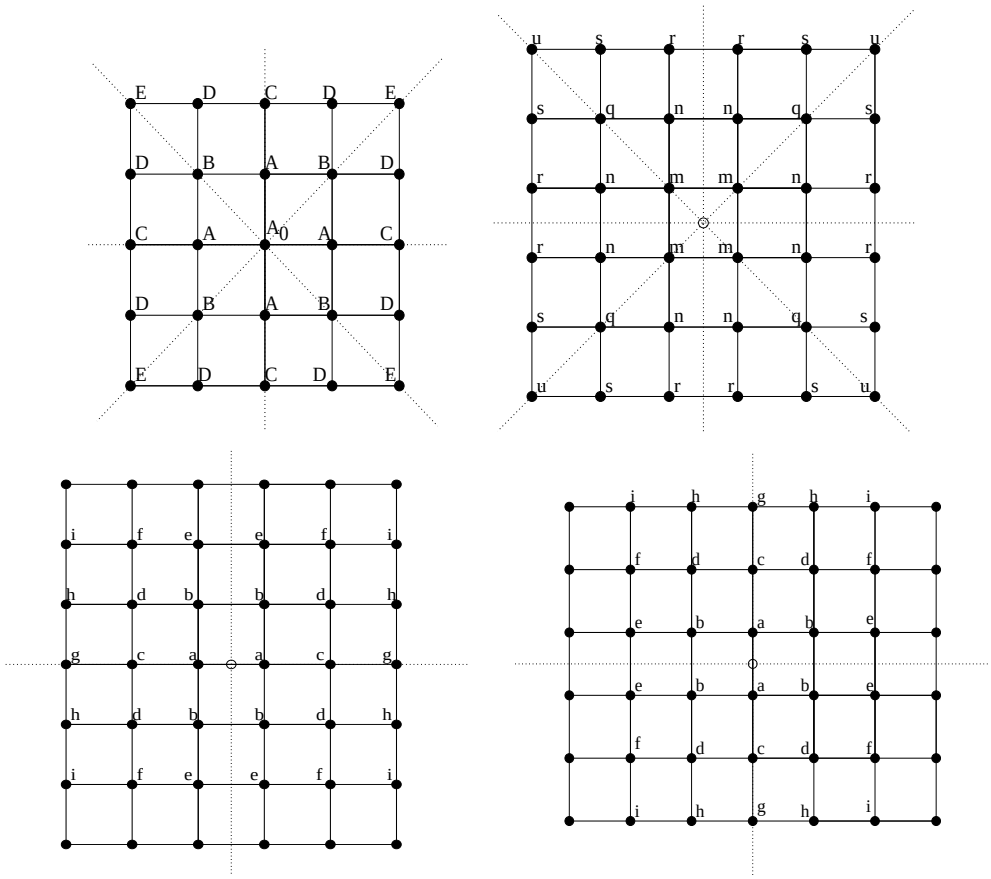

Figure 12: SSTs for the quadrilateral mesh. (Note that the bottom 2 templates are identical)

Definition 2 *The matrix-valued templates of a subdivision scheme are said to be symmetric subdivision templates* (SSTs)*, if the following conditions are satisfied:*

(1) *Each old vertex has the same template, and each new vertex of the same type (such as edge point or face point for the quadrilateral mesh) has the same template; and*

(2) *all the subdivision templates satisfy the following symmetry properties:*

(2.1) *For the 1-to-4 subdivision scheme of the quadrilateral mesh, the templates for the old vertices and new face vertices satisfy the four-directional symmetry property as shown on the top of Fig. 12; the template for the new edge vertices satisfies the two-directional symmetry property as shown in the bottom of Fig. 12.*

(2.2) *For the $\sqrt{2}$ subdivision scheme, the templates for both the old and new vertices satisfy the four-directional symmetry property shown on the top of Fig. 12.*

(2.3) *For the 1-to-4 subdivision scheme of a triangular mesh, the template for the old vertices satisfies the six-directional symmetry property as shown on the top-left of Fig. 13; and the template for the new vertices satisfies the two-directional symmetry property, as shown in Fig. 13.*

(2.4) *For the $\sqrt{3}$ subdivision scheme, the template for the old vertices satisfies the six-directional symmetry property shown on the top of Fig. 14, and the template for the*

new vertices satisfies the three-directional symmetry property as shown in the bottom of Fig. 14.

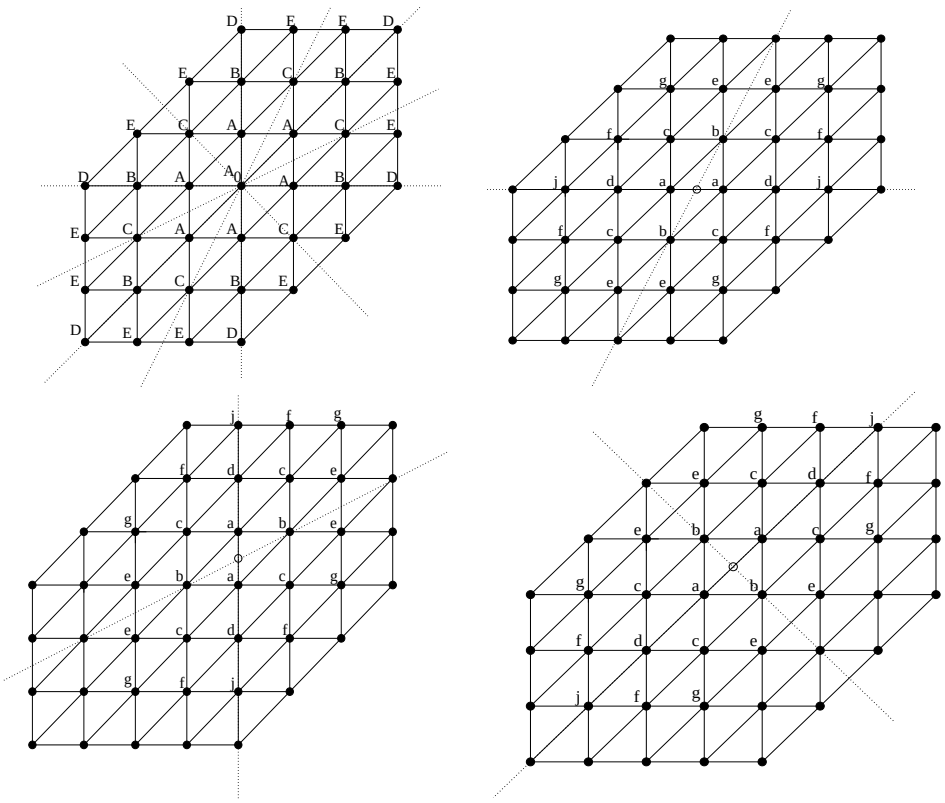

Figure 13: SSTs for the triangular mesh. (Note that when displayed on the equivalent triangular grid, the last 3 templates for generating new vertices are identical)

Theorem 1 (a) *The mask* $\{P_{\mathbf{k}}\}$ *of a 1-to-4 split subdivision scheme for the triangular mesh generates SSTs if and only if* $\{P_{\mathbf{k}}\}$ *satisfies the symmetry property* (2.18).

(b) *The mask* $\{P_{\mathbf{k}}\}$ *of a* $\sqrt{3}$ *subdivision generates SSTs if and only if* $\{P_{\mathbf{k}}\}$ *satisfies the symmetry property* (2.18).

Theorem 2 (a) *The mask* $\{P_{\mathbf{k}}\}$ *of a 1-to-4 split subdivision for the quadrilateral mesh generates SSTs if and only if* $\{P_{\mathbf{k}}\}$ *satisfies the symmetry property* (2.17).

(b) *The mask* $\{P_{\mathbf{k}}\}$ *of a* $\sqrt{2}$ *subdivision generates SSTs if and only if* $\{P_{\mathbf{k}}\}$ *satisfies the symmetry property* (2.17).

Proof of Theorem 1 (a): First assume that the templates associated with $\{P_{\mathbf{k}}\}$ are SSTs. Let $\widetilde{\mathbf{v}}_{\mathbf{k}}$ denote the vectors obtained after applying one subdivision iteration, namely:

$$\widetilde{\mathbf{v}}_{\mathbf{k}} = \sum_{\mathbf{j}} \mathbf{v}_{\mathbf{j}} P_{\mathbf{k}-2\mathbf{j}},$$

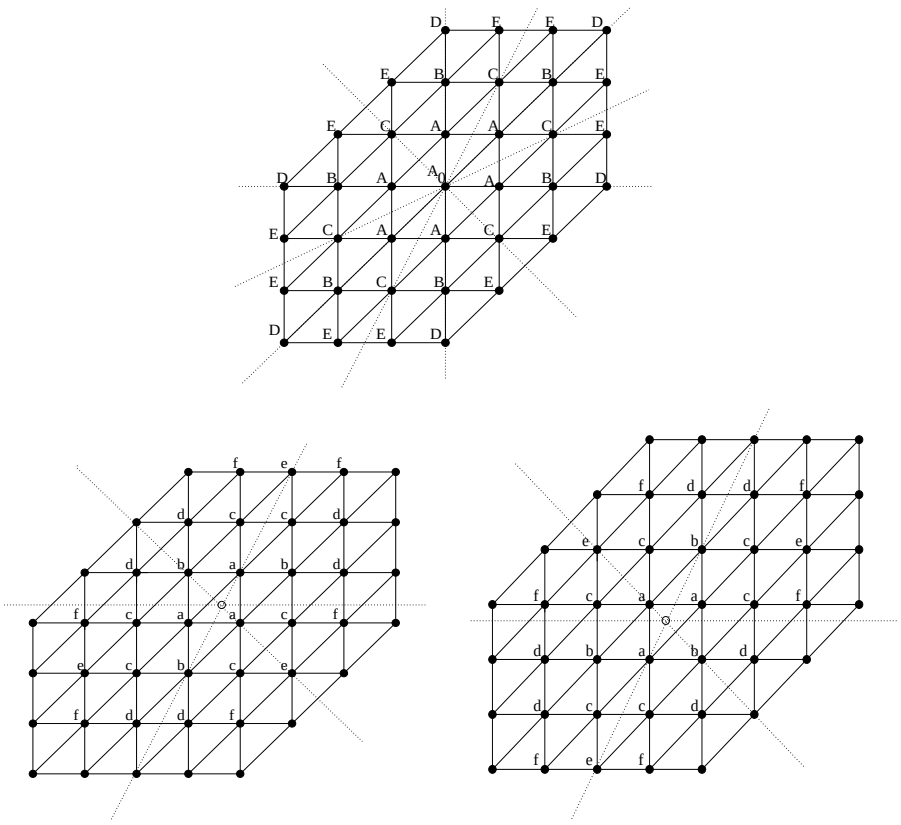

Figure 14: SSTs for the $\sqrt{3}$ subdivision. (Note that when displayed on the equivalent triangular grid, the last 2 templates for generating new vertices are identical)

with the previous vectors $\mathbf{v_k}$. Then the vectors corresponding to the old vertices are the vectors

$$\widetilde{\mathbf{v}}_{2\mathbf{k}} = \sum_{\mathbf{j}} \mathbf{v}_{\mathbf{j}} P_{2\mathbf{k}-2\mathbf{j}} = \sum_{\mathbf{j}} \mathbf{v}_{\mathbf{k}+\mathbf{j}} P_{-2\mathbf{j}}.$$

By the property of SSTs for the old vertices, we have that

$$P_{-2\mathbf{j}} = P_{-2T_1\mathbf{j}} = P_{-2T_2\mathbf{j}} = P_{2T_1\mathbf{j}} = P_{2T_2\mathbf{j}} = P_{2T_5\mathbf{j}} = P_{-2T_5\mathbf{j}}.$$

Thus (2.18) holds for all $\mathbf{k} \in 2\mathbb{Z}^2$.

On the other hand, the vectors corresponding to the new vertices are given by

$$\widetilde{\mathbf{v}}_{(1,0)+2\mathbf{k}} = \sum_{\mathbf{j}} \mathbf{v}_{\mathbf{k}+\mathbf{j}} P_{(1,0)-2\mathbf{j}},\ \widetilde{\mathbf{v}}_{(0,1)+2\mathbf{k}} = \sum_{\mathbf{j}} \mathbf{v}_{\mathbf{k}+\mathbf{j}} P_{(0,1)-2\mathbf{j}},\ \widetilde{\mathbf{v}}_{(1,1)+2\mathbf{k}} = \sum_{\mathbf{j}} \mathbf{v}_{\mathbf{k}+\mathbf{j}} P_{(1,1)-2\mathbf{j}}.$$

The SSTs property for the new vertices implies that

$$P_{(1,0)-2\mathbf{j}} = P_{(1,0)-2T_2\mathbf{j}} = P_{(1,0)-2(-T_2\mathbf{j}+(1,0))} = P_{(0,1)-2(-T_4\mathbf{j})} = P_{(1,1)-2T_3\mathbf{j}}, \tag{2.19}$$

where the last two equalities follow, since the template weights for the vertical and horizontal edge vertices, and as well as the vertices on the line with slope=1, are the same. Thus

$$P_{(1,0)-2\mathbf{j}} = P_{T_2((1,0)-2\mathbf{j})},$$

and

$$P_{T_1((1,0)-2\mathbf{j})} = P_{(1,1)-2T_1\mathbf{j}} = P_{(1,0)-2T_3^{-1}T_1\mathbf{j}} = P_{(1,0)-2T_2\mathbf{j}} = P_{(1,0)-2\mathbf{j}},$$

where the second and the last equalities follow from (2.19). Therefore, (2.18) holds for all $\mathbf{k}$ with $\mathbf{k} \in (1,0) + 2\mathbb{Z}^2$. Similarly, one can easily show that (2.18) holds for all $\mathbf{k}$ with $\mathbf{k} \in (0,1) + 2\mathbb{Z}^2$ and $\mathbf{k} \in (1,1) + 2\mathbb{Z}^2$. Hence, (2.18) holds for all $\mathbf{k} \in \mathbb{Z}^2$.

It is clear from the above proof that if $\{P_\mathbf{k}\}$ satisfies the symmetry property (2.18), then it yields templates that are SSTs. $\diamond$

Proof of Theorem 1 (b): First assume that the templates associated with $\{P_\mathbf{k}\}$ are SSTs. Let

$$\widetilde{\mathbf{v}}_\mathbf{k} = \sum_\mathbf{j} \mathbf{v}_\mathbf{j} P_{\mathbf{k}-A_1\mathbf{j}}$$

be the vectors obtained after one subdivision iteration with previous vectors $\{\mathbf{v}_\mathbf{k}\}$. Then the vectors corresponding to the old vertices in the next level of iteration are

$$\widetilde{\mathbf{v}}_{A_2\mathbf{k}} = \sum_\mathbf{j} \mathbf{v}_\mathbf{j} P_{A_1\mathbf{k}-A_1\mathbf{j}} = \sum_\mathbf{j} \mathbf{v}_{\mathbf{k}+\mathbf{j}} P_{-A_1\mathbf{j}}.$$

By the SSTs property of the template for the old vertices, we have

$$P_{A_1\mathbf{j}} = P_{A_1T_1\mathbf{j}} = P_{A_1T_2\mathbf{j}}.$$

Since

$$A_1T_1 = T_2A_1,\ A_1T_2 = T_1A_1, \tag{2.20}$$

we see that

$$P_{A_1\mathbf{j}} = P_{T_1A_1\mathbf{j}} = P_{T_2A_1\mathbf{j}}.$$

Thus (2.18) holds for $\mathbf{k} \in A_1\mathbb{Z}^2$.

On the other hand, the vectors corresponding to the new vertices are given by

$$\widetilde{\mathbf{v}}_{(1,0)+A_1\mathbf{k}} = \sum_\mathbf{j} \mathbf{v}_{\mathbf{k}+\mathbf{j}} P_{(1,0)-A_1\mathbf{j}}, \quad \widetilde{\mathbf{v}}_{(0,-1)+A_1\mathbf{k}} = \sum_\mathbf{j} \mathbf{v}_{\mathbf{k}+\mathbf{j}} P_{(0,-1)-A_1\mathbf{j}}.$$

By the SSTs property of the template for the new vertices, we have

$$P_{(1,0)-A_1\mathbf{j}} = P_{(1,0)-A_1T_1\mathbf{j}} = P_{(1,0)-A_1(-T_2\mathbf{j}+(1,0))} = P_{(1,0)-A_1(-T_5\mathbf{j}+(1,1))} = P_{(0,-1)-A_1T_3\mathbf{j}}, \tag{2.21}$$

where the last equality follows, since the template weights for the new face vertices of the both types of triangles are the same. The first equality of (2.21), together with (2.20), leads to

$$P_{(1,0)-A_1\mathbf{j}} = P_{(1,0)-T_2A_1\mathbf{j}} = P_{T_2((1,0)-A_1\mathbf{j})}. \tag{2.22}$$

On the other hand,

$$\begin{aligned} P_{T_1((1,0)-A_1\mathbf{j})} &= P_{(1,1)-T_1A_1\mathbf{j}} = P_{(0,-1)+(1,2)-A_1T_2\mathbf{j}} = P_{(0,-1)-A_1((0,1)+T_2\mathbf{j})} \\ &= P_{(1,0)-A_1T_3^{-1}((0,1)+T_2\mathbf{j})} = P_{(1,0)-A_1((1,1)-T_5\mathbf{j})} = P_{(1,0)-A_1\mathbf{j}}, \end{aligned} \tag{2.23}$$

where the first and the third equlaities in (2.23) follow from (2.21). Thus we have

$$P_{(1,0)-A_1\mathbf{j}} = P_{T_1((1,0)-A_1\mathbf{j})}. \tag{2.24}$$

Therefore, (2.18) holds for all $\mathbf{k} \in (1,0) + A_1\mathbb{Z}^2$. Similiary, one can easily show that (2.18) holds for all $\mathbf{k} \in (0,-1) + A_1\mathbb{Z}^2$. Since the union of $A_1\mathbb{Z}^2$, $(1,0) + A_1\mathbb{Z}^2$, and $(0,-1) + A_1\mathbb{Z}^2$ is all of $\mathbb{Z}^2$, (2.18) holds for all $\mathbf{k} \in \mathbb{Z}^2$.

We note that it is clear from the above proof that if $\{P_\mathbf{k}\}$ satisfies the symmetry property (2.18), then it provides templates that are SSTs. $\diamond$

Proof of Theorem 2 (a): First assume that the templates associated with $\{P_\mathbf{k}\}$ are SSTs. Let

$$\widetilde{\mathbf{v}}_\mathbf{k} = \sum_\mathbf{j} \mathbf{v}_\mathbf{j} P_{\mathbf{k}-2\mathbf{j}}$$

be the vectors obtained after one subdivision iteration with previous vectors $\{\mathbf{v}_\mathbf{k}\}$. Then the vectors corresponding to the old vertices in the next level of iteration are

$$\widetilde{\mathbf{v}}_{2\mathbf{k}} = \sum_\mathbf{j} \mathbf{v}_\mathbf{j} P_{2\mathbf{k}-2\mathbf{j}} = \sum_\mathbf{j} \mathbf{v}_{\mathbf{k}+\mathbf{j}} P_{-2\mathbf{j}}.$$

By the SSTs property of the template for the old vertices, we have

$$P_{-2\mathbf{j}} = P_{-2S_1\mathbf{j}} = P_{-2S_2\mathbf{j}} = P_{-2S_3\mathbf{j}} = P_{2S_3\mathbf{j}}.$$

Thus (2.17) holds for $\mathbf{k} \in 2\mathbb{Z}^2$.

On the other hand, the vectors corresponding to the new face vertices in the next level of iteration are

$$\widetilde{\mathbf{v}}_{(1,1)+2\mathbf{k}} = \sum_\mathbf{j} \mathbf{v}_\mathbf{j} P_{(1,1)+2\mathbf{k}-2\mathbf{j}} = \sum_\mathbf{j} \mathbf{v}_{\mathbf{k}+\mathbf{j}} P_{(1,1)-2\mathbf{j}}.$$

The SSTs property of the template for the new face vertices implies that

$$P_{(1,1)-2\mathbf{j}} = P_{(1,1)-2(S_2\mathbf{j}+(1,0))} = P_{(1,1)-2S_3\mathbf{j}} = P_{(1,1)-2(S_1\mathbf{j}+(0,1))} = P_{(1,1)-2(-S_3\mathbf{j}+(1,1))}.$$

That is,

$$P_{(1,1)-2\mathbf{j}} = P_{S_2((1,1)-2\mathbf{j})} = P_{S_3((1,1)-2\mathbf{j})} = P_{S_1((1,1)-2\mathbf{j})} = P_{-S_3((1,1)-2\mathbf{j})}.$$

Thus (2.17) holds for all $\mathbf{k}$ with $\mathbf{k} \in (1,1) + 2\mathbb{Z}^2$.

The vectors corresponding to the new horizontal edge vertices in the next level of iteration are

$$\widetilde{\mathbf{v}}_{(1,0)+2\mathbf{k}} = \sum_\mathbf{j} \mathbf{v}_\mathbf{j} P_{(1,0)+2\mathbf{k}-2\mathbf{j}} = \sum_\mathbf{j} \mathbf{v}_{\mathbf{k}+\mathbf{j}} P_{(1,0)-2\mathbf{j}},$$

and the vectors corresponding to the new vertical edge vertices in the next level of iteration are

$$\widetilde{\mathbf{v}}_{(0,1)+2\mathbf{k}} = \sum_\mathbf{j} \mathbf{v}_\mathbf{j} P_{(0,1)+2\mathbf{k}-2\mathbf{j}} = \sum_\mathbf{j} \mathbf{v}_{\mathbf{k}+\mathbf{j}} P_{(0,1)-2\mathbf{j}}.$$

The SSTs property of the template for the edge vertices implies that

$$P_{(1,0)-2\mathbf{j}} = P_{(1,0)-2(S_2\mathbf{j}+(1,0))} = P_{(1,0)-2S_1\mathbf{j}} = P_{(0,1)-2S_3\mathbf{j}},$$

where the last equality follows, since the templates for the horizontal and vertical edge vertices are the same. Thus

$$P_{(1,0)-2\mathbf{j}} = P_{S_2((1,0)-2\mathbf{j})} = P_{S_1((1,0)-2\mathbf{j})} = P_{S_3((1,0)-2\mathbf{j})}.$$

Therefore, (2.17) holds for all $\mathbf{k}$ with $\mathbf{k} \in (1,0) + 2\mathbb{Z}^2$. One can show similarly that (2.17) holds for all $\mathbf{k}$ with $\mathbf{k} \in (0,1) + 2\mathbb{Z}^2$. Hence (2.17) holds for all $\mathbf{k} \in \mathbb{Z}^2$.

It is clear from the above proof that if $\{P_\mathbf{k}\}$ satisfies the symmetry property (2.17), then it yields templates that are SSTs. $\diamond$

Proof of Theorem 2 (b): First assume that the templates associated with $\{P_\mathbf{k}\}$ are SSTs. Let

$$\widetilde{\mathbf{v}}_\mathbf{k} = \sum_\mathbf{j} \mathbf{v}_\mathbf{j} P_{\mathbf{k}-A_2\mathbf{j}}$$

be the vectors obtained after one subdivision iteration. Then the vectors corresponding to the old vertices in the next level of iteration are

$$\widetilde{\mathbf{v}}_{A_2\mathbf{k}} = \sum_\mathbf{j} \mathbf{v}_\mathbf{j} P_{A_2\mathbf{k}-A_2\mathbf{j}} = \sum_\mathbf{j} \mathbf{v}_{\mathbf{k}+\mathbf{j}} P_{-A_2\mathbf{j}}.$$

By the SSTs property of the templates for the old vertices, we have

$$P_{A_2\mathbf{j}} = P_{A_2S_1\mathbf{j}} = P_{A_2S_2\mathbf{j}} = P_{A_2S_3\mathbf{j}} = P_{-A_2S_3\mathbf{j}}.$$

Since

$$A_2S_1 = S_3A_2, \quad A_2S_3 = S_1A_2, \quad A_2S_2 = -S_3A_2, \tag{2.25}$$

we have

$$P_{A_2\mathbf{j}} = P_{S_3A_2\mathbf{j}} = P_{-S_3A_2\mathbf{j}} = P_{S_1A_2\mathbf{j}} = P_{S_2A_2\mathbf{j}}.$$

Thus (2.17) holds for $\mathbf{k} \in A_2\mathbb{Z}^2$.

The vectors corresponding to the new vertices in the next level of iteration are

$$\widetilde{\mathbf{v}}_{(1,0)+A_2\mathbf{k}} = \sum_\mathbf{j} \mathbf{v}_\mathbf{j} P_{(1,0)+A_2\mathbf{k}-A_2\mathbf{j}} = \sum_\mathbf{j} \mathbf{v}_{\mathbf{k}+\mathbf{j}} P_{(1,0)-A_2\mathbf{j}}.$$

By the SSTs property of the template for the new vertices, we have

$$P_{(1,0)-A_2\mathbf{j}} = P_{(1,0)-A_2(S_2\mathbf{j}+(1,0))} = P_{(1,0)-A_2(S_1\mathbf{j}+(0,1))} = P_{(1,0)-A_2S_3\mathbf{j}} = P_{(1,0)-A_2(-S_3\mathbf{j}+(1,1))}.$$

This and (2.25) lead to

$$P_{(1,0)-A_2\mathbf{j}} = P_{-S_3((1,0)-A_2\mathbf{j})} = P_{S_3((1,0)-A_2\mathbf{j})} = P_{S_1((1,0)-A_2\mathbf{j})} = P_{S_2((1,0)-A_2\mathbf{j})}.$$

Therefore, (2.17) holds for all $\mathbf{k} \in (1,0) + A_2\mathbb{Z}^2$. Since the union of $A_2\mathbb{Z}^2$ and $(1,0) + A_2\mathbb{Z}^2$ is all of $\mathbb{Z}^2$, (2.17) holds for all $\mathbf{k} \in \mathbb{Z}^2$.

We note that it is clear from the above proof that if $\{P_\mathbf{k}\}$ satisfies the symmetry property (2.17), then it provides templates that are SSTs. $\diamond$

In the following, we derive the symmetry properties of a refinable function (or distribution) vector Φ that corresponds to subdivision templates that are SSTs.

Theorem 3 *Let $\Phi = [\phi_0, \cdots, \phi_{r-1}]^T$ be a compactly supported refinable function (or distribution) vector with subdivision mask $\{P_{\mathbf{k}}\}$ and dilation matrix $A = 2I_2$ or $A = A_1$ in* (1.2)*. If the mask $\{P_{\mathbf{k}}\}$ satisfies* (2.18)*, then Φ satisfies*

$$\phi_\ell(\mathbf{x}) = \phi_\ell(T_1\mathbf{x}) = \phi_\ell(T_2\mathbf{x}),\ \mathbf{x} \in \mathbb{R}^2, \tag{2.26}$$

for each $\ell, \ell = 0, \cdots, r-1$.

Theorem 4 *Let $\Phi = [\phi_0, \cdots, \phi_{r-1}]^T$ be a compactly supported refinable function (or distribution) vector with subdivision mask $\{P_{\mathbf{k}}\}$ and dilation matrix $A = 2I_2$ or $A = A_2$ in* (1.2)*. If the mask $\{P_{\mathbf{k}}\}$ satisfies* (2.17)*, then Φ satisfies*

$$\phi_\ell(\mathbf{x}) = \phi_\ell(S_1\mathbf{x}) = \phi_\ell(S_2\mathbf{x}) = \phi_\ell(S_3\mathbf{x}),\ \mathbf{x} \in \mathbb{R}^2, \tag{2.27}$$

for each $\ell, \ell = 0, \cdots, r-1$.

As explained above, for ϕ_ℓs to satisfy the symmetry property (2.27), it must be 4-directional symmetric, as shown on the left of Fig. 11. Similarly, for ϕ_ℓ to satisfy the symmetry property (2.26), it must be 6-directional symmetric, as shown in the middle of Fig. 11. Set $\tilde{\phi}_\ell(\mathbf{x}) := \phi_\ell(\begin{bmatrix} 1 & \frac{1}{2} \\ 0 & 1 \end{bmatrix} \mathbf{x})$. Denote

$$\widetilde{T}_1 := \begin{bmatrix} 1 & \frac{1}{2} \\ 0 & 1 \end{bmatrix}^{-1} T_1 \begin{bmatrix} 1 & \frac{1}{2} \\ 0 & 1 \end{bmatrix} = \begin{bmatrix} \frac{1}{2} & \frac{3}{4} \\ 1 & -\frac{1}{2} \end{bmatrix}$$

$$\widetilde{T}_2 := \begin{bmatrix} 1 & \frac{1}{2} \\ 0 & 1 \end{bmatrix}^{-1} T_2 \begin{bmatrix} 1 & \frac{1}{2} \\ 0 & 1 \end{bmatrix} = \begin{bmatrix} 1 & 0 \\ & -1 \end{bmatrix}.$$

Then $\tilde{\phi}_\ell(\widetilde{T}_1\mathbf{x}) = \tilde{\phi}_\ell(\mathbf{x}), \tilde{\phi}_\ell(\widetilde{T}_2\mathbf{x}) = \tilde{\phi}_\ell(\mathbf{x})$. Thus $\tilde{\phi}_\ell$ satisfies the 6-directional symmetry property as shown on the right of Fig. 11. When constructing (scalar) 1-to-4 split subdivision schemes [30], and $\sqrt{3}$-subdivision schemes [21], the authors considered the symmetry of type (2.26) for the masks (hence for refinable functions). Here each component ϕ_ℓ of the refinable function vector Φ satisfies the symmetry property of type (2.26) or of type (2.27).

The proofs of Theorem 3 and Theorem 4 are similar, and it is easier to consider the dilation matrix $A = 2I_2$ than the dilation matrices $A = A_1$ and $A = A_2$. Furthermore, the proof of the theorems for the dilation matrices $A = A_1$ and $A = A_2$ are also similar. Hence, in the following we only give the proof of Theorem 4 for $A = A_2$.

Proof of Theorem 4 with $A = A_2$. Let $P(\omega)$ be the two-scale symbol of the mask $\{P_{\mathbf{k}}\}$ defined by (2.7) with $A = A_2$. Then Φ is given by (2.9) with $A = A_2$, i.e.,

$$\widehat{\Phi}(\omega) = \Pi_{n=1}^{\infty} P(A_2^{-n}\omega)\mathbf{u}_0,$$

since $A_2^T = A_2$, where $\mathbf{u}_0$ is an eigenvector associated with the eigenvalue 1 of $P(0)$.

On one hand, (2.17) implies that

$$P(S_i\omega) = P(\omega),\ i = 1, 2, 3.$$

On the other hand, it is easy to verify that $A_2^{-1}S_1 = S_3A_2^{-1}$, and $A_2^{-2}S_1 = S_1A_2^{-2}$. Thus, $A_2^{-n}S_1$ is either $S_3A_2^{-n}$ or $S_1A_2^{-n}$. In either case, $P(A_2^{-n}S_1\omega)$ is the same as $P(A_2^{-n}\omega)$, since $P(S_1A_2^{-n}\omega) = P(S_3A_2^{-n}\omega) = P(A_2^{-n}\omega)$. Therefore, we have

$$\widehat{\Phi}(S_1\omega) = \Pi_{n=1}^{\infty}P(A_2^{-n}S_1\omega)\mathbf{u}_0 = \Pi_{n=1}^{\infty}P(A_2^{-n}\omega)\mathbf{u}_0 = \widehat{\Phi}(\omega);$$

that is, $\Phi(S_1\mathbf{x}) = \Phi(\mathbf{x})$. Similarly, by $A_2^{-1}S_2 = S_1S_2S_3A_2^{-1}$ and $A_2^{-1}S_3 = S_1A_2^{-1}$ respectively, we have $\Phi(S_2\mathbf{x}) = \Phi(\mathbf{x})$ and $\Phi(S_3\mathbf{x}) = \Phi(\mathbf{x})$. This shows that $\phi_\ell, 0 \le \ell \le r-1$, satisfy the symmetry properties (2.27). $\diamond$

3. Construction of symmetric interpolatory subdivision templates (SISTs)

In this section, we will describe a procedure for constructing matrix-valued subdivision templates for interpolatory surface subdivisions, and give examples of C^2 templates for both triangular and quadrilateral nets, demonstrating each of the 1-to-4 split, $\sqrt{3}$, and $\sqrt{2}$ topological rules. Since this paper is concerned only with regular vertices, the bulk of the work is in the construction of the corresponding subdivision masks. In practice, only low-dimensional matrices are of interest to us. Hence, the examples we will derive are matrix-valued subdivision masks $\{P_{\mathbf{k}}\}$ of dimensions $r = 2$ and $r = 3$ for C^2 interpolatory surface subdivisions. It will become obvious that larger values of the dimension r allow more free parameters for constructing subdivision templates for generating 3-D surfaces with a higher order of smoothness.

For the matrix-valued subdivision templates to be SSTs, the masks $\{P_{\mathbf{k}}\}$ to be constructed must satisfy (2.18) or (2.17), so that the corresponding function vectors Φ satisfy the symmetry properties (2.26) or (2.27), for triangular or quadrilateral meshes, respectively. Furthermore, since we are concerned with C^2-subdivision schemes, it is convenient to construct subdivision masks $\{P_{\mathbf{k}}\}$ that satisfy the so-called "sum rule" of order 4, which implies that Φ locally reproduces all polynomials of total degree 3. (See, for example, [19, 17, 20] for the notion of sum rules and the same reference for a computational method for meeting the requirement of any desirable sum rule order.)

The general procedure suggested in this paper is to formulate a subdivision mask $\{P_{\mathbf{k}}\}$ that satisfies the interpolatory condition (2.12) and the symmetry properties (2.18) or (2.17), starting with the smallest support, but large enough so that there is enough freedom for the matrix entries to accommodate the requirement of the sum rule of order 4. Then a set of linear equations is formulated, with the matrix entries that have not yet been determined as unknowns, by imposing the requirement of the sum rule of order 4. The template size must be large enough for the existence of solutions, or else the matrix dimension r can be increased from 2 to 3 or even higher. We prefer, however, small values of r, and are happy to point out that r=2 is sufficient in general. The

general solution of the equations are formulated in terms of some free parameters, which are to be adjusted by applying the algorithm/software in [18]/[20] to meet the desirable order of smoothness. Again, increasing the support or the matrix dimension r might be needed if the desirable order of smoothness is larger than 2. As mentioned above, for C^2 interpolatory subdivisions, r=2 is large enough for the "minimum" template size in general.

In the consideration of the order of smoothness, we will compute the Sobolev exponents s. More precisely, let $s \geq 0$ and denote by W^s the Sobolev space consisting of functions $f(\mathbf{x})$ on $\mathbb{R}^2$ with

$$\int_{\mathbf{R}^2} (1 + |\omega|^2)^s |\hat{f}(\omega)|^2 d\omega < \infty,$$

where $\hat{f}$ denotes the Fourier transform of f. Observe that by the Sobolev embedding theorem, for $s > n+1$, a function in W^s is necessarily in C^n, meaning that all its partial derivatives of orders up to n are continuous. In this paper, for a function vector Φ, by writing $\Phi \in W^s$, we mean that each component of Φ is in W^s. Since we are only interested in subdivision schemes that are at least C^2, all refinable function vectors Φ to be derived in this paper are in W^s with $s > 3$. We use the smoothness formula in [18] to compute the Sobolev exponent estimates.

We also remark that while a similar matrix transformation, applied to change the geometric performance of a symmetric subdivision mask, preserves the property of SSTs, it does not alter the smoothness property of the corresponding refinable function vector. More precisely, for dimension $r = 2$ or 3 considered in the following examples, let

$$U = \begin{bmatrix} 1 & * \\ 0 & * \end{bmatrix} \quad \text{or} \quad U = \begin{bmatrix} 1 & * & * \\ 0 & * & * \\ 0 & * & * \end{bmatrix}, \tag{3.1}$$

be any non-singular constant matrix. Then if a subdivision mask $\{P_{\mathbf{k}}\}$ is interpolatory and satisfies certain appropriate symmetry properties, then $\{UP_{\mathbf{k}}U^{-1}\}$ is again an interpolatory subdivision mask that also satisfies the same symmetry property. The corresponding refinable function vector is given by $U\Phi$, whose components are only linear transformations of that of Φ.

Of course, the purpose of introducing this similar matrix transformation is to change the functionality of the shape control parameters, as can be seen from the transformed refinable function vector $U\Phi$. In practice, U should be chosen according to the need of the user. However, since we are only concerned with the issue of smoothness in this paper, we will simply set U to be the identity matrix.

Returning to the vector-valued refinement equation (2.1), where the refinable function vector Φ satisfies (2.2), with the first component of $\mathbf{w}$ satisfying (2.3), we will choose the vector $\mathbf{w}$ to be $[1,\ 0]$ for $r = 2$ and $[1,\ 0,\ 0]$ for $r = 3$, in all the examples to be presented in the following subsections.

3.1 C^2-interpolatory schemes for triangular meshes

In this subsection, we demonstrate the application of the procedure described above to compute matrix-valued subdivision templates for triangular meshes. Both the 1-to-4 split and $\sqrt{3}$ subdivisions are demonstrated.

3.1.1 Interpolatory 1-to-4 split subdivision schemes

We first derive a family of interpolatory masks $\{P_{\mathbf{k}}\}$ that generate SISTs and satisfy the sum rule of order 4:

$$P_{0,0} = \begin{bmatrix} 1 & \frac{3}{2}t_3 + 9t_4 - \frac{3}{8} \\ 0 & t_3 \end{bmatrix}, \tag{3.2}$$

$$P_{1,0} = P_{1,1} = P_{0,1} = P_{-1,0} = P_{-1,-1} = P_{0,-1} = B, \tag{3.3}$$

$$P_{2,1} = P_{1,2} = P_{-1,1} = P_{-2,-1} = P_{-1,-2} = P_{1,-1} = C, \tag{3.4}$$

$$P_{2,0} = P_{-2,0} = P_{0,2} = P_{0,-2} = P_{2,2} = P_{-2,-2} = D, \tag{3.5}$$

where

$$B = \begin{bmatrix} \frac{3}{8} & 0 \\ -\frac{1}{8} - t_1 & \frac{1}{8} - t_2 \end{bmatrix},$$

$$C = \begin{bmatrix} \frac{1}{8} & 0 \\ t_1 & t_2 \end{bmatrix},$$

$$D = \begin{bmatrix} 0 & \frac{1}{16} - \frac{1}{4}t_3 - \frac{3}{2}t_4 \\ 0 & t_4 \end{bmatrix},$$

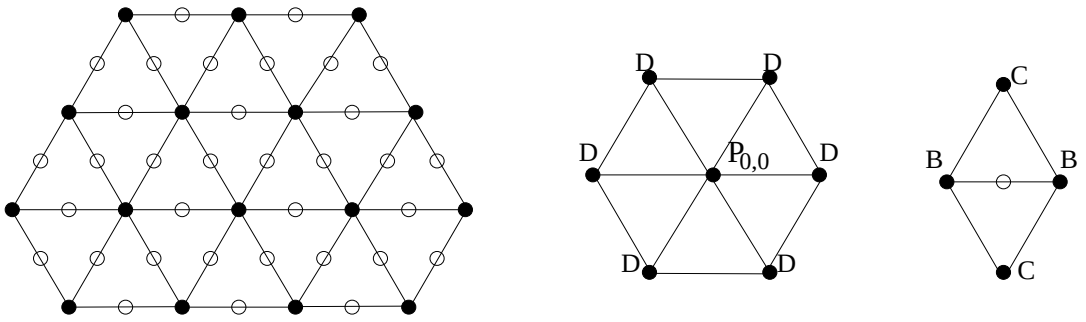

Figure 15: Subdivion templates for the local averaging rule of C^2 interpolatory 1-to-4 split subdivision scheme

See Fig. 15 for the subdivision templates. Note that the sizes of the templates are the same as those of the Loop scheme in Fig. 6. Also note that the $(1,1)$-entries of B, C are the same as the weights $\frac{3}{8}, \frac{1}{8}$ of the Loop scheme. (This is also the case for $r = 3$.)

For the choice of

$$t_1 = -0.03295922922033, \quad t_2 = -0.01031166415430,$$
$$t_3 = -0.35533104771638, \quad t_4 = -0.08729664374763,$$

Figure 16: Interpolatory refinable function vector components: ϕ_0 (on left) and ϕ_1 (on right)

the corresponding refinable function vector $\Phi = [\phi_0, \phi_1]^T$ is in $W^{3.03532}$. If we choose

$$[t_1, \cdots, t_4] = \frac{1}{512}[-17,\ -5,\ -182,\ -45], \tag{3.6}$$

the resulting Φ is in $W^{3.03450}$. See Fig. 16 for the pictures of the two components of Φ with the parameters t_js given in (3.6).

For $r = 3$, let $P_{0,0}$ be the matrix defined by (3.7) and the other nonzero matrices of the mask be given by (3.3), (3.4), (3.5) with B, C, D as follows:

$$P_{0,0} = \begin{bmatrix} 1 & \frac{3}{2}t_{12} + 9t_{16} & \frac{3}{2}t_{13} + 9t_{17} - \frac{3}{8} \\ 0 & t_{10} & t_{11} \\ 0 & t_{12} & t_{13} \end{bmatrix}, \tag{3.7}$$

$$B = \begin{bmatrix} \frac{3}{8} & 0 & 0 \\ t_1 & t_2 & t_3 \\ -\frac{1}{8} - t_7 & -t_8 & \frac{1}{8} - t_9 \end{bmatrix},$$

$$C = \begin{bmatrix} \frac{1}{8} & 0 & 0 \\ t_4 & t_5 & t_6 \\ t_7 & t_8 & t_9 \end{bmatrix},$$

$$D = \begin{bmatrix} 0 & -\frac{1}{4}t_{12} - \frac{3}{2}t_{16} & \frac{1}{16} - \frac{1}{4}t_{13} - \frac{3}{2}t_{17} \\ 0 & t_{14} & t_{15} \\ 0 & t_{16} & t_{17} \end{bmatrix},$$

There are 17 free parameters in this family. For an appropriate choice of $t_1, \cdots, t_{17}$ (the numerical values of t_js are not provided here), the resulting Φ is in $W^{3.162644}$. If we choose the numerical values:

$$[t_1,\ \cdots,\ t_{17}] = \frac{1}{1024}[14,\ 6,\ 9,\ 89,\ -13,\ -183,\ -37,\ 5,\ 2,$$
$$14,\ 54,\ -49,\ -352,\ -18,\ 152,\ -2,\ -95],$$

then the resulting Φ is in $W^{3.16183}$.

3.1.2 Interpolatory $\sqrt{3}$-subdivision schemes

For $r = 2$, we derive a family of $\sqrt{3}$-subdivision interpolatory masks $\{G_{\mathbf{k}}\}$ that generate SISTs and satisfy the sum rule of order 4:

$$G_{0,0} = \begin{bmatrix} 1 & 18t_3 + 3t_4 - 1 \\ 0 & t_4 \end{bmatrix}, \tag{3.8}$$

$$G_{1,0} = G_{1,1} = G_{0,1} = G_{-1,0} = G_{-1,-1} = G_{0,-1} = X, \tag{3.9}$$

$$G_{2,0} = G_{-2,0} = G_{0,2} = G_{0,-2} = G_{2,2} = G_{-2,-2} = Y, \tag{3.10}$$

$$G_{2,1} = G_{1,2} = G_{-1,1} = G_{-2,-1} = G_{-1,-2} = G_{1,-1} = W, \tag{3.11}$$

where

$$X = \begin{bmatrix} \frac{8}{27} & 0 \\ -\frac{4}{81} - t_1 & \frac{1}{9} - t_2 \end{bmatrix},$$

$$Y = \begin{bmatrix} \frac{1}{27} & 0 \\ t_1 & t_2 \end{bmatrix},$$

$$W = \begin{bmatrix} 0 & \frac{1}{6} - 3t_3 - \frac{1}{2}t_4 \\ 0 & t_3 \end{bmatrix},$$

See Fig. 17 for the subdivision templates, and observe that the template size for new vertices here is even smaller than that in [24] for C^1 scalar interpolatory $\sqrt{3}$-subdivision scheme.

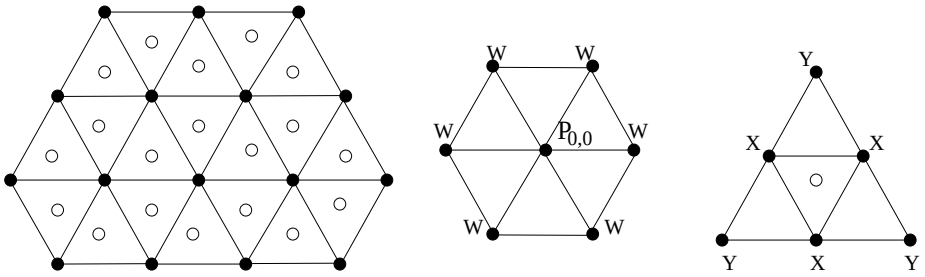

Figure 17: Subdivision templates for the local averaging rule for C^2 interpolatory $\sqrt{3}$-subdivision scheme

For the choice of

$$t_1 = -0.00688446701758, \quad t_2 = -0.01078888570421,$$
$$t_3 = -0.11334594212367, \quad t_4 = -0.29446533980366,$$

the refinable function vector $\Phi = [\phi_0, \phi_1]^T$ is in $W^{3.80780}$; while if we choose

$$[t_1, \cdots, t_4] = -\frac{1}{81 \times 16}[9,\ 14,\ 147,\ 382], \tag{3.12}$$

Figure 18: Interpolatory refinable function vector: ϕ_0 (on left) and ϕ_1 (on right)

the resulting Φ is in $W^{3.80778}$. See Fig. 18 for the pictures of the two components of Φ with the parameters t_js given in (3.12).

For $r = 3$, let $G_{0,0}$ be the matrix defined by (3.13) and the other nonzero matrices of the mask be given by (3.9), (3.10), (3.11) with X, Y, W as follows:

$$G_{0,0} = \begin{bmatrix} 1 & 9t_{10} + \frac{3}{2}t_{14} - \frac{1}{2} & 9t_{11} + \frac{3}{2}t_{15} \\ 0 & t_{14} & t_{15} \\ 0 & t_{16} & t_{17} \end{bmatrix}, \tag{3.13}$$

$$X = \begin{bmatrix} \frac{8}{27} & 0 & 0 \\ t_1 & t_2 & t_3 \\ t_4 & t_5 & t_6 \end{bmatrix},$$

$$Y = \begin{bmatrix} \frac{1}{27} & 0 & 0 \\ -\frac{8}{81} - t_1 & \frac{1}{9} - t_2 & -t_3 \\ t_7 & t_8 & t_9 \end{bmatrix},$$

$$W = \begin{bmatrix} 0 & \frac{1}{12} - \frac{3}{2}t_{10} - \frac{1}{4}t_{14} & -\frac{3}{2}t_{11} - \frac{1}{4}t_{15} \\ 0 & t_{10} & t_{11} \\ 0 & t_{12} & t_{13} \end{bmatrix},$$

We may choose $t_1, \cdots, t_{17}$ so that the resulting $\Phi = [\phi_0, \phi_1, \phi_2]^T$ is in $W^{3.92864}$ (again, the numerical values of t_js are not provided here). With the choice of

$$[t_1, \cdots, t_{17}] = \frac{1}{81 \times 16}[-110,\ 129,\ 16,\ -236,\ 328,\ -2,\ -31,\ -56,\ 12,\ -58,\ -36,\ -146,\ -71,\ -142,\ -105,\ -171,\ -207],$$

the corresponding Φ is in $W^{3.92212}$.

3.2 C^2-Interpolatory schemes for quadrilateral meshes

In this subsection, we demonstrate our procedure by deriving C^2-interpolatory 1-to-4 split and 4-to-8 (i.e.$\sqrt{2}$) subdivision templates for the quadrilateral mesh.

3.2.1 Interpolatory 1-to-4 split subdivision schemes

We give a family of interpolatory masks $\{R_{\mathbf{k}}\}$ that generate SISTs and satisfy the sum rule of order 4:

$$R_{0,0} = \begin{bmatrix} 1 & r_{1,2} \\ 0 & t_6 \end{bmatrix}, \quad r_{1,2} = \frac{1}{2} + 4t_3 - 8t_4 - 8t_5 - 2t_6, \tag{3.14}$$

$$R_{1,0} = R_{0,1} = R_{-1,0} = R_{0,-1} = J, \tag{3.15}$$

$$R_{1,1} = R_{1,-1} = R_{-1,1} = R_{-1,-1} = K, \tag{3.16}$$

$$R_{2,0} = R_{-2,0} = R_{0,2} = R_{0,-2} = L, \tag{3.17}$$

$$R_{2,1} = R_{1,2} = R_{-1,-2} = R_{-2,-1} = R_{2,-1} = R_{-2,1} = R_{-1,2} = R_{1,-2} = M, \tag{3.18}$$

$$R_{2,2} = R_{-2,2} = R_{2,-2} = R_{-2,-2} = N, \tag{3.19}$$

where

$$J = \begin{bmatrix} \frac{3}{8} & 0 \\ \frac{1}{8} - 2t_1 & \frac{1}{8} - 2t_2 \end{bmatrix},$$

$$K = \begin{bmatrix} \frac{1}{4} & 0 \\ \frac{1}{16} & \frac{1}{16} \end{bmatrix},$$

$$L = \begin{bmatrix} 0 & -t_3 - \frac{1}{4}r_{1,2} \\ 0 & t_5 \end{bmatrix},$$

$$M = \begin{bmatrix} \frac{1}{16} & 0 \\ t_1 & t_2 \end{bmatrix},$$

$$N = \begin{bmatrix} 0 & t_3 \\ 0 & t_4 \end{bmatrix},$$

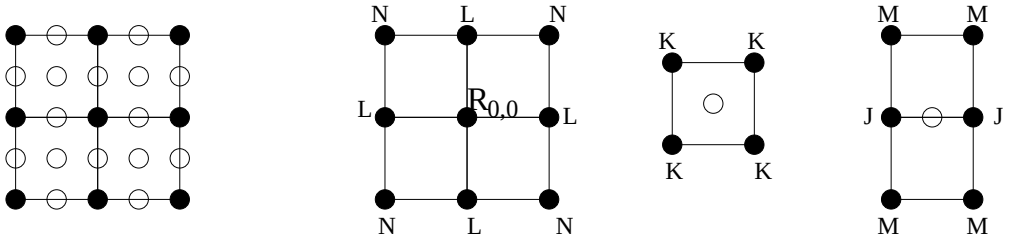

Figure 19: Subdivision templates for the local averaging rule of C^2 interpolatory 1-to-4 split subdivision scheme

See Fig. 19 for the subdivision templates, and observe that their sizes are the same as those of the Catmull-Clark scheme in Fig. 7. Also note that the $(1,1)$-entry of K agrees with the weight $\frac{1}{4}$ in the Catmull-Clark scheme in the averaging rule for the (new) face vertices and that the $(1,1)$-entries of J, M are exactly the same as the weights $\frac{3}{8}, \frac{1}{16}$ in the Catmull-Clark scheme in the averaging rule for the (new) edge vertices. (This is also the case for $r = 3$.)

Next, we choose $t_1, \cdots, t_6$ so that the resulting $\Phi = [\phi_0, \phi_1]^T$ is in $W^{3.27720}$ (the numerical values of t_js are not provided here). For the choice of

$$[t_1,\ \cdots,\ t_6] = \frac{1}{256}[5,\ -1,\ -30,\ -9,\ -33,\ -86], \tag{3.20}$$

the corresponding Φ is in $W^{3.27323}$. See Fig. 20 for the refinable function vector with components ϕ_0 (on the left) and $-\phi_1$ (on the right), with t_js given by (3.20).

Figure 20: Interpolatory refinable functions ϕ_0 (on left) and $-\phi_1$ (on right)

For $r = 3$, we may consider $R_{0,0}$ to be the matrix defined by (3.21) and the other nonzero matrices of the mask given by (3.15)-(3.19) with J, K, L, M, N given below:

$$R_{0,0} = \begin{bmatrix} 1 & \tilde{r}_{1,2} & \tilde{r}_{1,3} \\ 0 & t_{23} & t_{24} \\ 0 & t_{25} & t_{26} \end{bmatrix}, \tag{3.21}$$

$$J = \begin{bmatrix} \frac{3}{8} & 0 & 0 \\ t_1 & t_2 & t_3 \\ -\frac{1}{8} - 2t_{10} & -2t_{11} & \frac{1}{8} - 2t_{12} \end{bmatrix},$$

$$K = \begin{bmatrix} \frac{1}{4} & 0 & 0 \\ t_4 & t_5 & t_6 \\ -\frac{1}{16} & 0 & \frac{1}{16} \end{bmatrix},$$

$$L = \begin{bmatrix} 0 & -t_{17} - \frac{1}{4}\tilde{r}_{1,2} & -t_{18} - \frac{1}{4}\tilde{r}_{1,3} \\ 0 & t_{13} & t_{14} \\ 0 & t_{15} & t_{16} \end{bmatrix},$$

$$M = \begin{bmatrix} \frac{1}{16} & 0 & 0 \\ t_7 & t_8 & t_9 \\ t_{10} & t_{11} & t_{12} \end{bmatrix}, \quad N = \begin{bmatrix} 0 & t_{17} & t_{18} \\ 0 & t_{19} & t_{20} \\ 0 & t_{21} & t_{22} \end{bmatrix},$$

where

$$\tilde{r}_{1,2} = 4(2t_{15} + 2t_{21} + t_{25} + t_{17}), \quad \tilde{r}_{1,3} = 4(2t_{16} + 2t_{22} + t_{26} + t_{18}) - \frac{1}{2}.$$

We may choose some appropriate t_js so that the resulting Φ is in $W^{3.56225}$ (the numerical values of t_js are not provided here). For the choice of

$$[t_1, \cdots, t_{26}] = \frac{1}{512}[-28,\ 12,\ 40,\ -16,\ 16,\ 28,\ -4,\ -4,\ -2,\ -\frac{45}{4},\ 0,\ \frac{5}{2}$$
$$-12,\ -32,\ -20,\ -58,\ 0,\ 64,\ 0,\ -8,\ -4,\ -21,\ -56,\ -96,\ -48,\ -144],$$

the resulting Φ is in $W^{3.52612}$.

3.2.2 Interpolatory $\sqrt{2}$-subdivision schemes

We now derive a family of interpolatory masks $\{L_{\mathbf{k}}\}$ that generate SISTs and satisfy the sum rule of order 4, namely:

$$L_{0,0} = \begin{bmatrix} 1 & 8t_1 + 2t_2 - 1 \\ 0 & t_2 \end{bmatrix}, \tag{3.22}$$
$$L_{1,0} = L_{0,1} = L_{-1,0} = L_{0,-1} = H, \tag{3.23}$$
$$L_{1,1} = L_{1,-1} = L_{-1,1} = L_{-1,-1} = I, \tag{3.24}$$

where

$$H = \begin{bmatrix} \frac{1}{4} & 0 \\ -\frac{1}{16} & \frac{1}{8} \end{bmatrix},$$
$$I = \begin{bmatrix} 0 & \frac{1}{4} - 2t_1 - \frac{1}{2}t_2 \\ 0 & t_1 \end{bmatrix}.$$

See Fig. 21 for the subdivision templates. If we choose $t_1 = -0.15911662281039, t_2 = 0.10323661586963$, the resulting Φ is in $W^{3.18743}$; if $t_1 = -\frac{5}{32}, t_2 = \frac{1}{8}$, Φ is in $W^{3.17794}$; and if $t_1 = -\frac{1}{8}, t_2 = \frac{1}{8}$, then Φ is in $W^{3.05094}$. See Fig. 22 for the refinable function vector with components ϕ_0 (on the left) and ϕ_1 (on the right), for $t_1 = -\frac{5}{32}, t_2 = \frac{1}{8}$.

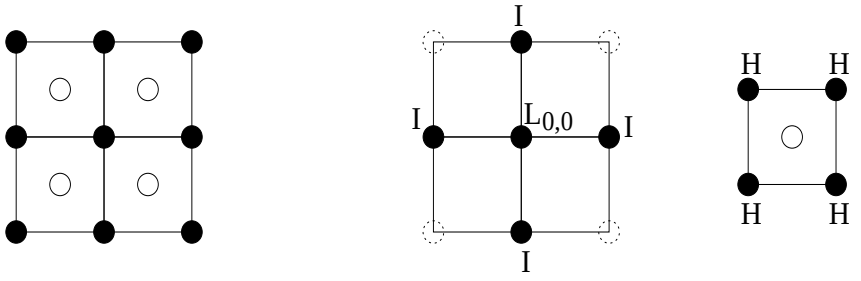

Figure 21: Subdivision templates for the local averaging rule of C^2 interpolatory $\sqrt{2}$-subdivision scheme

Figure 22: Interpolatory refinable function vector with components: ϕ_0 (on left) and ϕ_1 (on right)

For $r = 3$, let $L_{0,0}$ be the matrix in (3.25) and the other nonzero matrices of the mask be defined by (3.23), (3.24), with H, I given below:

$$L_{0,0} = \begin{bmatrix} 1 & \frac{1}{2} - 4t_4 - t_8 & -4t_5 - t_9 \\ 0 & t_8 & t_9 \\ 0 & t_{10} & t_{11} \end{bmatrix}, \tag{3.25}$$

$$H = \begin{bmatrix} \frac{1}{4} & 0 & 0 \\ \frac{1}{8} & \frac{1}{8} & 0 \\ t_1 & t_2 & t_3 \end{bmatrix},$$

$$I = \begin{bmatrix} 0 & t_4 + \frac{1}{4}t_8 - \frac{1}{8} & t_5 + \frac{1}{4}t_9 \\ 0 & t_4 & t_5 \\ 0 & t_6 & t_7 \end{bmatrix}.$$

For the choice of

$$[t_1, \cdots, t_{11}] = \frac{1}{512}[20,\ -46,\ 2,\ -90,\ 31,\ -54,\ -15,\ 36,\ -16,\ 70,\ -36],$$

the resulting Φ is in $W^{3.92491}$.

4. C^2 Spline interpolatory subdivision schemes

Suppose we are already given a refinable function vector Φ associated with an approximation, but not interpolatory, subdivision scheme. If Φ is a very desirable function vector, such as C^2 bivariate splines that locally reproduce polynomials of total degree at least 3 and have very small supports and explicit formulations, say, in terms of Bézier coefficients, it is very tempting just to modify Φ by taking a linear combination of the integer translates of its components to preserve the knowledge of the Bézier coefficients, in order to achieve the interpolation property, as long as the supports are enlarged, if necessary, only by a little. Hence, instead of introducing parameters in the matrix entries of some unknown subdivision mask, we only apply the interpolation and symmetry

rules (2.16) and (2.17) or (2.18) to find a suitable linear combination. Therefore, the procedure described in the previous section is simplified significantly. In particular, there is no need to impose the fourth order sum rule requirement and to find the Sobolev exponents to verify for the order of smoothness. We demonstrate this simplified procedure by giving two examples in this section.

4.1 C^2-cubic spline interpolatory schemes

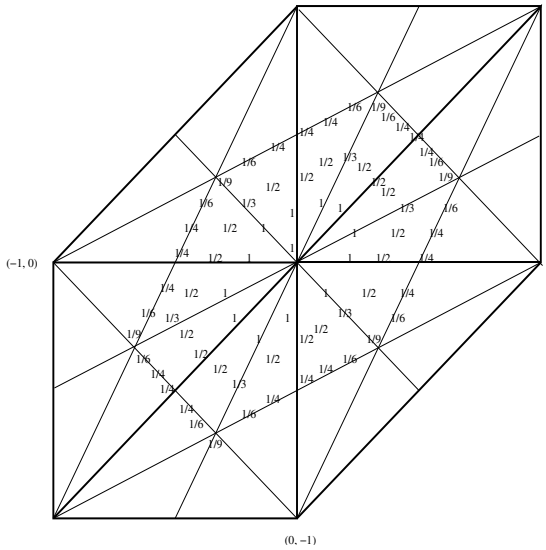

Figure 23: Support and Bézier coefficients of ϕ_0^b

Let ϕ_0^b be the C^2 cubic spline introduced in [3] with its support and Bézier coefficients shown in Fig. 23, where the zero coefficients are not displayed. Define

$$\phi_1^b := \phi_0^b(A_1^{-1}\cdot),$$

where A_1 is the dilation matrix in (1.2). See Fig. 24 for the support and the Bézier coefficients of ϕ_1^b, where only a portion of the Bézier coefficients are displayed due to the six-directional symmetry property of ϕ_1^b. It was shown in [3] that $\Phi^b := [\phi_0^b,\ \phi_1^b]^T$ is refinable with both dilation matrix $A = 2I_2$ and dilation matrix $A = A_1$, and its corresponding subdivision masks are calculated in [3] with the symbols P_{2I_2} and P_{A_1} given by

$$P_{2I_2}(\omega) := \frac{1}{32}\begin{bmatrix} -1+p(\mathbf{z}) & 9 \\ 1+\frac{2}{3}p(\mathbf{z})+\frac{1}{3}p(\mathbf{z}^2)+\frac{1}{3}q(\mathbf{z}) & 5+3p(\mathbf{z})+q(\mathbf{z}) \end{bmatrix},$$
$$P_{A_1}(\omega) := \frac{1}{3}\begin{bmatrix} 0 & 1 \\ \frac{1}{9}+\frac{2}{27}p(\mathbf{z})+\frac{1}{27}p(\mathbf{z}^2)+\frac{1}{27}q(\mathbf{z}) & \frac{2}{3}+\frac{1}{3}p(\mathbf{z}) \end{bmatrix},$$

where $\omega = (\omega_1, \omega_2)$, $\mathbf{z} := (e^{-i\omega_1}, e^{-i\omega_2})$, $\mathbf{z}^2 := (e^{-i2\omega_1}, e^{-i2\omega_2})$, and

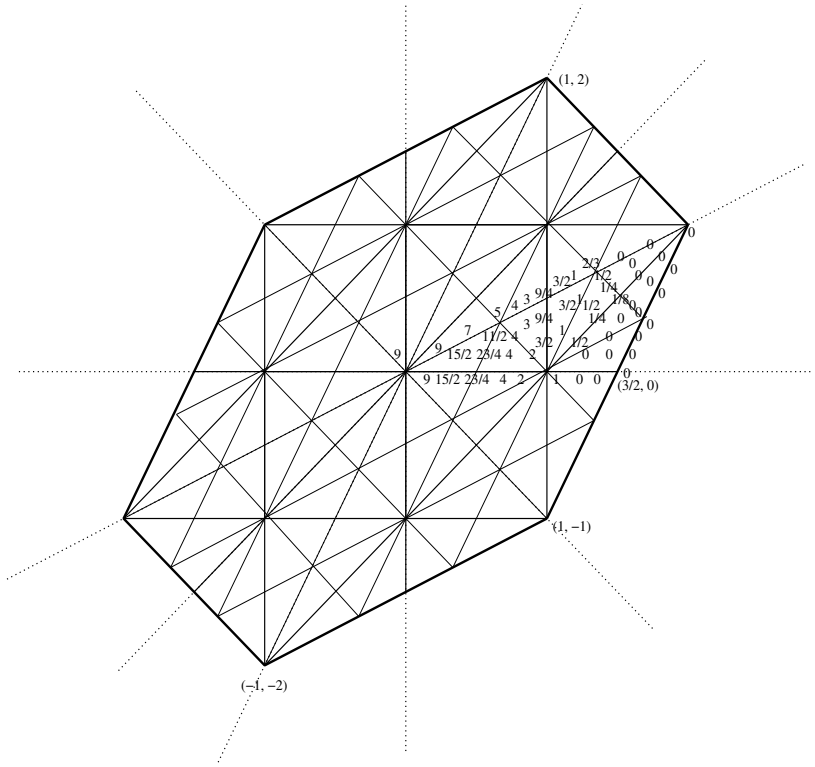

Figure 24: Support and Bézier coefficients of $9\phi_1^b$

$$p(\mathbf{z}) := z_1 + z_1^{-1} + z_2 + z_2^{-1} + z_1 z_2 + (z_1 z_2)^{-1}, \tag{4.1}$$
$$q(\mathbf{z}) := z_1^2 z_2 + z_1^{-2} z_2^{-1} + z_1 z_2^2 + z_1^{-1} z_2^{-2} + z_1 z_2^{-1} + z_1^{-1} z_2.$$

These masks with dilation matrices $A = 2I_2$ and $A = A_1$ yield SSTs for 1-to-4 split and $\sqrt{3}$-subdivision schemes, respectively. The sizes of the templates of the 1-to-4 split subdivision scheme are the same as those of the Loop scheme, see [3]. However, these schemes are not interpolatory. So, we modify ϕ_1^b so that the new subdivision schemes are interpolatory and remain SSTs. To do so, we define

$$\begin{aligned}\widetilde{\phi}_1^b := \phi_1^b - \phi_0^b - \frac{1}{9}\{&\phi_0^b(\cdot - (1,0)) + \phi_0^b(\cdot - (1,1)) + \phi_0^b(\cdot - (0,1)) \\ &+\phi_0^b(\cdot + (1,0)) + \phi_0^b(\cdot + (1,1)) + \phi_0^b(\cdot + (0,1))\},\end{aligned} \tag{4.2}$$

and consider

$$\widetilde{\Phi}^b := [\phi_0^b,\ 9\widetilde{\phi}_1^b]^T.$$

Then $\widetilde{\Phi}^b$ satisfies (2.16), and is still refinable with dilation matrices $2I_2$ and A_1. Thus the masks associated with dilation matrices $2I_2$ and A_1, denoted by $\{\widetilde{P}_\mathbf{k}\}$ and $\{\widetilde{G}_\mathbf{k}\}$ respectively, yield interpolatory 1-to-4 split and $\sqrt{3}$-subdivision schemes. One can easily find the the support and the Bézier coefficients of $\widetilde{\phi}_1^b$ from that for ϕ_0^b and ϕ_1^b. See Fig. 25 for the pictures of ϕ_0^b and $-9\widetilde{\phi}_1^b$.

Figure 25: Interpolatory refinable function vector with compnents: ϕ_0^b (on left), $-9\widetilde{\phi}_1^b$ (on right)

Denote

$$U_1(\omega_1,\omega_2) := \begin{bmatrix} 1 & 0 \\ -9-p(\mathbf{z}) & 9 \end{bmatrix}, \quad \mathbf{z} = (e^{-i\omega_1}, e^{-i\omega_2}),$$

where $p(\mathbf{z})$ is given in (4.1). Then by the relationship between Φ^b and $\widetilde{\Phi}^b$, namely: $\widehat{\widetilde{\Phi}}^b(\omega) = U_1(\omega)\widehat{\Phi}^b(\omega)$, we see that the symbols $\widetilde{P}(\omega)$ and $\widetilde{G}(\omega)$ for $\widetilde{\Phi}^b$ with dilation matrices $2I_2$ and A_1 are given respectively by

$$\widetilde{P}(\omega) = U_1(2\omega)P_{2I_2}(\omega)U_1(\omega)^{-1}, \quad \widetilde{G}(\omega) = U_1(A_1^T\omega)P_{A_1}(\omega)U_1(\omega)^{-1}.$$

It is easy to find the nonzero matrix-valued coefficients $\widetilde{P}_{\mathbf{k}}$, namely:

$$\begin{aligned}
&\widetilde{P}_{0,0} = \begin{bmatrix} 1 & \frac{1}{8} \\ 0 & -\frac{1}{2} \end{bmatrix}, \\
&\widetilde{P}_{1,0} = \widetilde{P}_{1,1} = \widetilde{P}_{0,1} = \widetilde{P}_{-1,0} = \widetilde{P}_{-1,-1} = \widetilde{P}_{0,-1} = B, \\
&\widetilde{P}_{2,1} = \widetilde{P}_{1,2} = \widetilde{P}_{-1,1} = \widetilde{P}_{-2,-1} = \widetilde{P}_{-1,-2} = \widetilde{P}_{1,-1} = C, \\
&\widetilde{P}_{2,0} = \widetilde{P}_{-2,0} = \widetilde{P}_{0,2} = \widetilde{P}_{0,-2} = \widetilde{P}_{2,2} = \widetilde{P}_{-2,-2} = D, \\
&\widetilde{P}_{3,1} = \widetilde{P}_{3,2} = \widetilde{P}_{2,3} = \widetilde{P}_{1,3} = \widetilde{P}_{-1,2} = \widetilde{P}_{-2,1} = \widetilde{P}_{-3,-1} = \\
&\qquad \widetilde{P}_{-3,-2} = \widetilde{P}_{-2,-3} = \widetilde{P}_{-1,-3} = \widetilde{P}_{1,-2} = \widetilde{P}_{2,-1} = E, \\
&\widetilde{P}_{3,0} = \widetilde{P}_{3,3} = \widetilde{P}_{0,3} = \widetilde{P}_{-3,0} = \widetilde{P}_{-3,-3} = \widetilde{P}_{0,-3} = F,
\end{aligned}$$

where

$$B = \begin{bmatrix} \frac{1}{4} & 0 \\ \frac{13}{4} & \frac{3}{8} \end{bmatrix}, \; C = \begin{bmatrix} 0 & 0 \\ \frac{7}{4} & \frac{1}{8} \end{bmatrix}, \; D = \begin{bmatrix} 0 & 0 \\ 0 & -\frac{1}{8} \end{bmatrix}, \; E = \begin{bmatrix} 0 & 0 \\ -\frac{1}{8} & 0 \end{bmatrix}, \; F = \begin{bmatrix} 0 & 0 \\ -\frac{1}{4} & 0 \end{bmatrix}$$

This mask $\{\widetilde{P}_{\mathbf{k}}\}$ yields immediately the subdivision templates, as shown in Fig. 26, for C^2 interpolatory 1-to-4 split subdivision scheme.

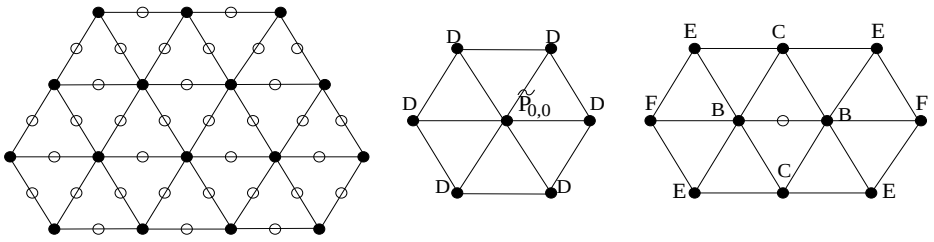

Figure 26: Subdivision template for the local averaging rule of C^2-cubic spline interpolatory 1-to-4 split subdivision scheme

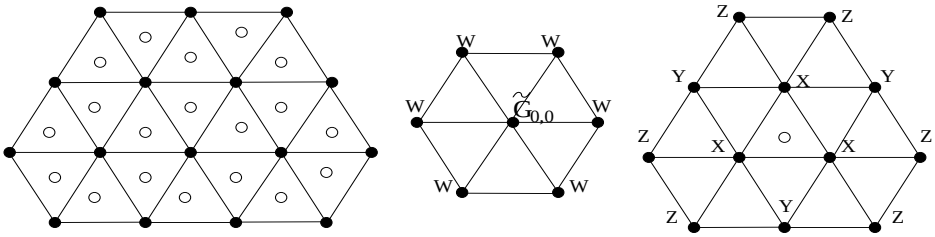

Figure 27: Subdivision templates for the local averaging rule of C^2-cubic spline interpolatory $\sqrt{3}$-subdivision

It is also easy to find the nonzero matrix-valued coefficients $\widetilde{G}_{\mathbf{k}}$, namely:

$$\begin{aligned}
&\widetilde{G}_{0,0} = \begin{bmatrix} 1 & \frac{1}{9} \\ 0 & -\frac{1}{3} \end{bmatrix}, \\
&\widetilde{G}_{1,0} = \widetilde{G}_{1,1} = \widetilde{G}_{0,1} = \widetilde{G}_{-1,0} = \widetilde{G}_{-1,-1} = \widetilde{G}_{0,-1} = X, \\
&\widetilde{G}_{2,1} = \widetilde{G}_{1,2} = \widetilde{G}_{-1,1} = \widetilde{G}_{-2,-1} = \widetilde{G}_{-1,-2} = \widetilde{G}_{1,-1} = W, \\
&\widetilde{G}_{2,0} = \widetilde{G}_{-2,0} = \widetilde{G}_{0,2} = \widetilde{G}_{0,-2} = \widetilde{G}_{2,2} = \widetilde{G}_{-2,-2} = Y, \\
&\widetilde{G}_{3,1} = \widetilde{G}_{3,2} = \widetilde{G}_{2,3} = \widetilde{G}_{1,3} = \widetilde{G}_{-1,2} = \widetilde{G}_{-2,1} = \widetilde{G}_{-3,-1} = \\
&\qquad \widetilde{G}_{-3,-2} = \widetilde{G}_{-2,-3} = \widetilde{G}_{-1,-3} = \widetilde{G}_{1,-2} = \widetilde{G}_{2,-1} = Z,
\end{aligned}$$

where

$$X = \begin{bmatrix} \frac{1}{9} & 0 \\ \frac{34}{9} & \frac{1}{3} \end{bmatrix}, \quad W = \begin{bmatrix} 0 & 0 \\ 0 & -\frac{1}{9} \end{bmatrix}, \quad Y = \begin{bmatrix} 0 & 0 \\ \frac{4}{9} & 0 \end{bmatrix}, \quad Z = \begin{bmatrix} 0 & 0 \\ -\frac{1}{9} & 0 \end{bmatrix}.$$

Similarly, the mask $\{\widetilde{G}_{\mathbf{k}}\}$ yields the subdivision templates, as shown in Fig. 27, for a C^2 interpolatory $\sqrt{3}$-subdivision scheme. Observe that the template size for the new vertices here is the same as that in [24] for C^1 scalar (non-spline) interpolatory $\sqrt{3}$-subdivision scheme.

4.2 C^2-quartic spline interpolatory schemes

Let ϕ_0^d be the C^2 quartic spline introduced in [6] with its support and Bézier coefficients shown in Fig. 28, where the zero coefficients are not displayed.

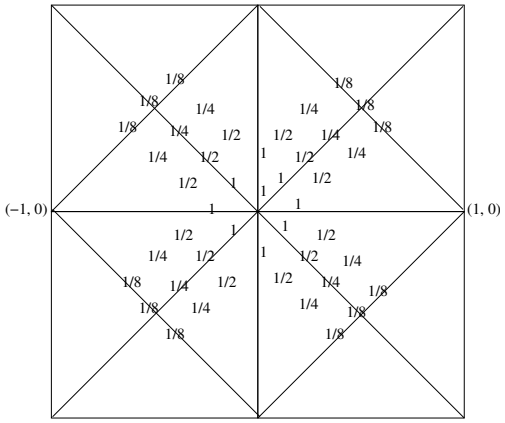

Figure 28: Support and Bézier coefficients of $\phi_0^d \in S_4^2(\triangle^2)$

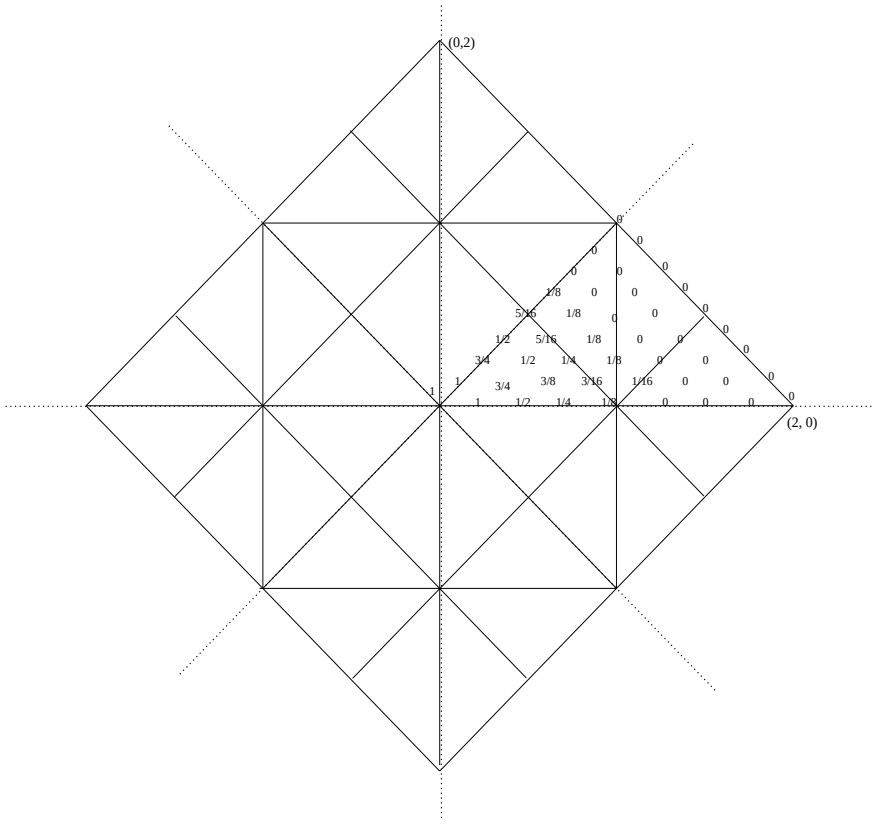

Figure 29: Support and Bézier coefficients of $\phi_1^d \in S_4^2(\triangle^2)$

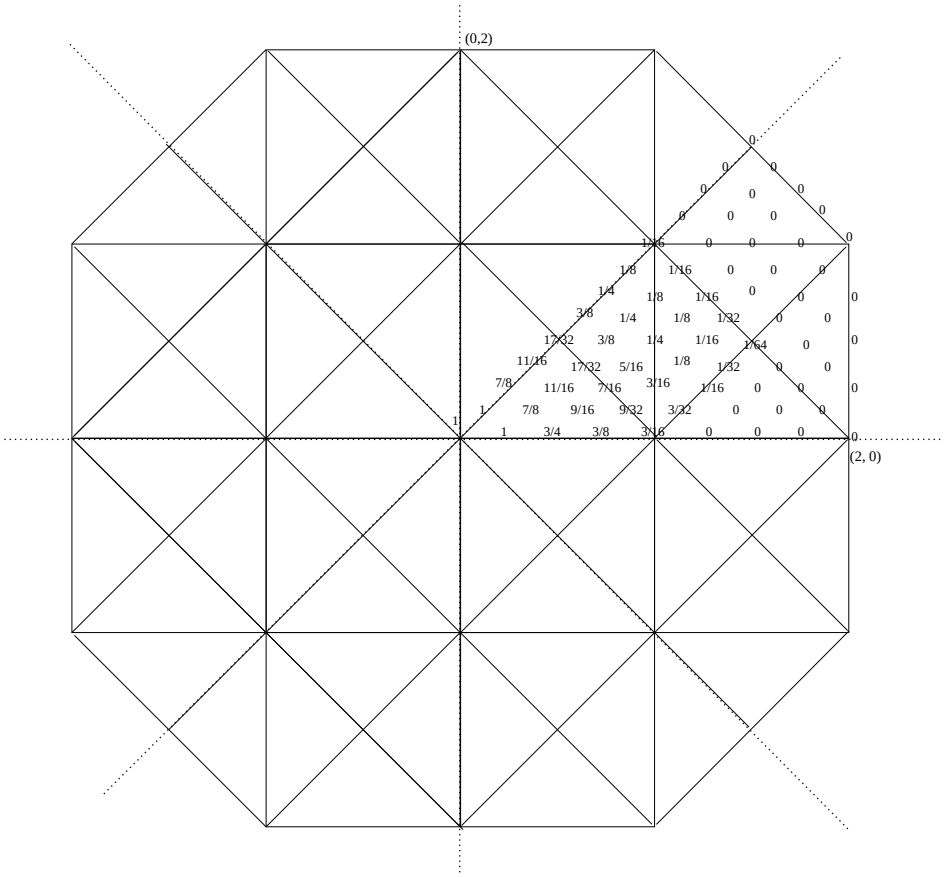

Figure 30: Support and Bézier coefficients of $\phi_2^d \in S_4^2(\triangle^2)$

Define

$$\phi_1^d := \phi_0^d(A_2^{-1}\cdot), \tag{4.3}$$

$$\begin{aligned}\phi_2^d := \phi_0^d(\frac{\cdot}{2}) - \frac{1}{8}\{&\phi_0^d(\cdot-(1,0)) + \phi_0^d(\cdot-(0,1)) + \phi_0^d(\cdot+(1,0)) + \phi_0^d(\cdot+(0,1))\} \\ -\frac{1}{16}\{&\phi_0^d(\cdot-(1,1)) + \phi_0^d(\cdot+(1,-1)) + \phi_0^d(\cdot+(1,1)) + \phi_0^d(\cdot-(1,-1))\},\end{aligned} \tag{4.4}$$

where A_2 is the dilation matrix given in (1.2). See Fig. 29 and Fig. 30 for the supports and Bézier coefficients of ϕ_1^d and ϕ_2^d, respectively, where only a portion of Bézier coefficients are displayed due to the four-directional symmetry of ϕ_1^d and ϕ_2^d. It was shown in [6] that $\Phi^d := [\phi_0^d,\ \phi_1^d,\ \phi_2^d]^T$ is refinable with both dilation matrix $A = 2I_2$ and dilation matrix $A = A_2$, and the corresponding subdivision masks are calculated in [6] with the symbols $R_{2I_2}(\omega)$ and $L_{A_2}(\omega)$ given by

$$\begin{aligned}R_{2I_2}(\omega) &= L_{A_2}(A_2\omega)L_{A_2}(\omega), \\ L_{A_2}(\omega) &= \frac{1}{32}\begin{bmatrix} 0 & 32 & 0 \\ 2(2r(\mathbf{z})+u(\mathbf{z})) & 0 & 32 \\ u(\mathbf{z}) & 4(2+r(\mathbf{z})) & 8(2+r(\mathbf{z})) \end{bmatrix},\end{aligned}$$

where again $\mathbf{z} := (e^{-i\omega_1}, e^{-i\omega_2})$, $\mathbf{z}^2 := (e^{-i2\omega_1}, e^{-i2\omega_2})$, and

$$r(\mathbf{z}) := z_1 + z_1^{-1} + z_2 + z_2^{-1}, \tag{4.5}$$
$$u(\mathbf{z}) := z_1 z_2 + (z_1 z_2)^{-1} + z_1 z_2^{-1} + z_1^{-1} z_2. \tag{4.6}$$

These masks yield SSTs for 1-to-4 split and $\sqrt{2}$ subdivisions. The sizes of the templates of the 1-to-4 split subdivision scheme are the same as those of the Catmull-Clark scheme (see [6]), but the schemes are not interpolatory. So, again we modify ϕ_1^d, ϕ_2^d so that the new subdivision schemes are interpolatory and remain SSTs. To do so, we define

$$\begin{aligned}\widetilde{\phi}_1^d := \phi_1^d - \phi_0^d - \frac{1}{8}\{&\phi_0^d(\cdot - (1,0)) + \phi_0^d(\cdot + (1,0)) \\ &+\phi_0^d(\cdot - (0,1)) + \phi_0^d(\cdot + (0,1))\},\end{aligned} \tag{4.7}$$

$$\begin{aligned}\widetilde{\phi}_2^d := \phi_2^d - \phi_0^d - \frac{3}{16}\{&\phi_0^d(\cdot - (1,0)) + \phi_0^d(\cdot + (1,0)) \\ &+\phi_0^d(\cdot - (0,1)) + \phi_0^d(\cdot + (0,1))\} \\ -\frac{1}{16}\{&\phi_0^d(\cdot - (1,1)) + \phi_0^d(\cdot + (1,-1)) + \phi_0^d(\cdot + (1,1)) + \phi_0^d(\cdot - (1,-1))\},\end{aligned} \tag{4.8}$$

and consider

$$\widetilde{\Phi}^d := [\phi_0^d,\ \widetilde{\phi}_1^d,\ \widetilde{\phi}_2^d]^T.$$

Then $\widetilde{\Phi}^d$ satisfies (2.16) and is still refinable with both of the dilation matrices $2I_2$ and A_2. Therefore, their subdivision masks immediately result in interpolatory 1-to-4 split and $\sqrt{2}$ subdivision schemes. One can easily find the Bézier coefficients for $\widetilde{\phi}_1^d$ and $\widetilde{\phi}_2^d$ from those for ϕ_0^d, ϕ_1^d, and ϕ_2^d. See Fig. 31 for the pictures of the components ϕ_0^d, $-\widetilde{\phi}_1^d$, and $-\widetilde{\phi}_2^d$.

Figure 31: Interpolatory refinable function vector with components: ϕ_0^d (on left), $-\widetilde{\phi}_1^d$ (in middle), $-\widetilde{\phi}_2^d$ (on right)

Denote

$$U_2(\omega_1, \omega_2) := \begin{bmatrix} 1 & 0 & 0 \\ -1 - r(\mathbf{z}) & 1 & 0 \\ -1 - \frac{3}{16} r(\mathbf{z}) - \frac{1}{16} u(\mathbf{z}) & 0 & 1 \end{bmatrix}, \quad \mathbf{z} = (e^{-i\omega_1}, e^{-i\omega_2}),$$

where $r(\mathbf{z})$ and $u(\mathbf{z})$ are given in (4.5) and (4.6). Then in view of the relationship between Φ^d and $\widetilde{\Phi}^d$ given by $\widehat{\widetilde{\Phi}}^d(\omega) = U_2(\omega)\widehat{\Phi}^d(\omega)$, we see that the symbols $\widetilde{R}(\omega)$ and $\widetilde{L}(\omega)$ for $\widetilde{\Phi}^d$ with dilation matrices $2I_2$ and A_2 are given, respectively, by

$$\widetilde{R}(\omega) = U_2(2\omega)R_{2I_2}(\omega)U_2(\omega)^{-1}, \quad \widetilde{L}(\omega) = U_2(A_2\omega)L_{A_2}(\omega)U_2(\omega)^{-1}.$$

It is easy to find the nonzero matrix-valued coefficients $\widetilde{R}_{\mathbf{k}}$, given by

$$\begin{aligned}
&\widetilde{R}_{0,0} = \begin{bmatrix} 1 & 0 & 1 \\ 0 & \frac{1}{4} & -\frac{1}{2} \\ 0 & \frac{1}{8} & -\frac{1}{2} \end{bmatrix}, \\
&\widetilde{R}_{1,0} = \widetilde{R}_{0,1} = \widetilde{R}_{-1,0} = \widetilde{R}_{0,-1} = J, \quad \widetilde{R}_{1,1} = \widetilde{R}_{1,-1} = \widetilde{R}_{-1,1} = \widetilde{R}_{-1,-1} = K, \\
&\widetilde{R}_{2,0} = \widetilde{R}_{-2,0} = \widetilde{R}_{0,2} = \widetilde{R}_{0,-2} = L, \\
&\widetilde{R}_{2,1} = \widetilde{R}_{1,2} = \widetilde{R}_{-1,-2} = \widetilde{R}_{-2,-1} = \widetilde{R}_{2,-1} = \widetilde{R}_{-2,1} = \widetilde{R}_{-1,2} = \widetilde{R}_{1,-2} = M, \\
&\widetilde{R}_{2,2} = \widetilde{R}_{-2,2} = \widetilde{R}_{2,-2} = \widetilde{R}_{-2,-2} = N, \quad \widetilde{R}_{3,0} = \widetilde{R}_{-3,0} = \widetilde{R}_{0,3} = \widetilde{R}_{0,-3} = O, \\
&\widetilde{R}_{3,1} = \widetilde{R}_{1,3} = \widetilde{R}_{-1,-3} = \widetilde{R}_{-3,-1} = \widetilde{R}_{3,-1} = \widetilde{R}_{-3,1} = \widetilde{R}_{-1,3} = \widetilde{R}_{1,-3} = Q, \\
&\widetilde{R}_{3,2} = \widetilde{R}_{2,3} = \widetilde{R}_{-2,-3} = \widetilde{R}_{-3,-2} = \widetilde{R}_{3,-2} = \widetilde{R}_{-3,2} = \widetilde{R}_{-2,3} = \widetilde{R}_{2,-3} = S, \\
&\widetilde{R}_{3,3} = \widetilde{R}_{-3,3} = \widetilde{R}_{3,-3} = \widetilde{R}_{-3,-3} = T,
\end{aligned}$$

where

$$\begin{aligned}
&J = \begin{bmatrix} \frac{5}{16} & 0 & 0 \\ \frac{7}{32} & \frac{1}{8} & \frac{1}{4} \\ \frac{21}{64} & \frac{1}{8} & \frac{1}{4} \end{bmatrix}, \quad K = \begin{bmatrix} \frac{1}{8} & 0 & 0 \\ \frac{5}{32} & \frac{1}{8} & 0 \\ \frac{45}{128} & \frac{1}{16} & \frac{1}{4} \end{bmatrix}, \quad L = \begin{bmatrix} 0 & 0 & 0 \\ 0 & \frac{1}{16} & -\frac{1}{8} \\ 0 & \frac{1}{32} & -\frac{3}{16} \end{bmatrix}, \\
&M = \begin{bmatrix} 0 & 0 & 0 \\ 0 & 0 & 0 \\ \frac{7}{64} & \frac{1}{32} & \frac{1}{16} \end{bmatrix}, \quad N = \begin{bmatrix} 0 & 0 & 0 \\ 0 & 0 & 0 \\ 0 & 0 & -\frac{1}{16} \end{bmatrix}, \quad O = \begin{bmatrix} 0 & 0 & 0 \\ -\frac{1}{32} & 0 & 0 \\ -\frac{3}{64} & 0 & 0 \end{bmatrix} \\
&Q = \begin{bmatrix} 0 & 0 & 0 \\ -\frac{1}{64} & 0 & 0 \\ -\frac{1}{64} & 0 & 0 \end{bmatrix}, \quad S = \begin{bmatrix} 0 & 0 & 0 \\ 0 & 0 & 0 \\ -\frac{1}{64} & 0 & 0 \end{bmatrix}, \quad T = \begin{bmatrix} 0 & 0 & 0 \\ 0 & 0 & 0 \\ -\frac{1}{128} & 0 & 0 \end{bmatrix}.
\end{aligned}$$

The subdivision templates of the local averaging rule of this interpolatory scheme are shown in Fig. 32.

We may also find the nonzero matrix-valued coefficients $\widetilde{L}_{\mathbf{k}}$ of the mask $\{\widetilde{L}_{\mathbf{k}}\}$ for $\widetilde{\Phi}^d$ with dilation matrix A_2, listed as follows:

$$\begin{aligned}
&\widetilde{L}_{0,0} = \begin{bmatrix} 1 & 1 & 0 \\ 0 & -1 & 1 \\ 0 & -\frac{3}{4} & \frac{1}{2} \end{bmatrix}, \\
&\widetilde{L}_{1,0} = \widetilde{L}_{0,1} = \widetilde{L}_{-1,0} = \widetilde{L}_{0,-1} = H, \\
&\widetilde{L}_{1,1} = \widetilde{L}_{1,-1} = \widetilde{L}_{-1,1} = \widetilde{L}_{-1,-1} = I, \\
&\widetilde{L}_{2,1} = \widetilde{L}_{1,2} = \widetilde{L}_{-1,-2} = \widetilde{L}_{-2,-1} = \widetilde{L}_{2-,1} = \widetilde{L}_{-2,1} = \widetilde{L}_{-1,2} = \widetilde{L}_{1,-2} = \widetilde{H}, \\
&\widetilde{L}_{2,0} = \widetilde{L}_{-2,0} = \widetilde{L}_{0,2} = \widetilde{L}_{0,-2} = \widetilde{I}, \\
&\widetilde{L}_{3,0} = \widetilde{L}_{-3,0} = \widetilde{L}_{0,3} = \widetilde{L}_{0,-3} = \widetilde{T},
\end{aligned}$$

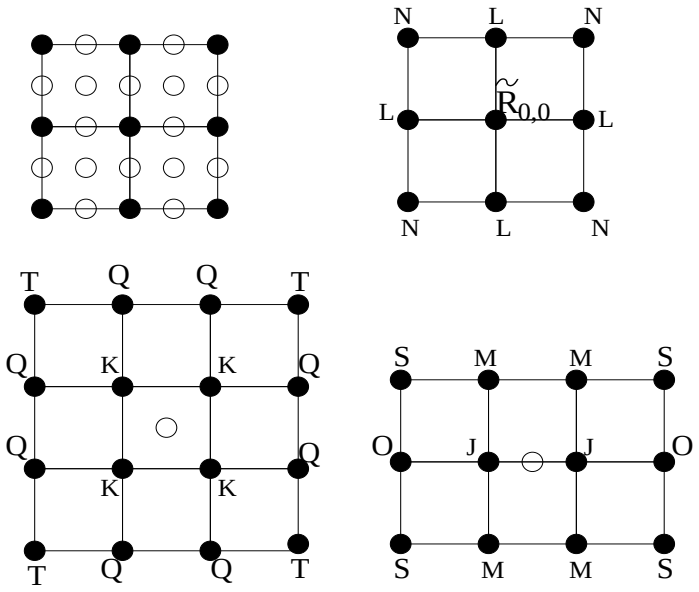

Figure 32: Subdivision templates for the local averaging rule of C^2-quartic spline interpolatory 1-to-4 split subdivision scheme

where

$$H = \begin{bmatrix} \frac{1}{8} & 0 & 0 \\ \frac{5}{32} & 0 & 0 \\ \frac{45}{128} & \frac{1}{8} & \frac{1}{4} \end{bmatrix}, \quad I = \begin{bmatrix} 0 & 0 & 0 \\ 0 & -\frac{1}{8} & 0 \\ 0 & -\frac{3}{16} & 0 \end{bmatrix}, \quad \widetilde{H} = \begin{bmatrix} 0 & 0 & 0 \\ -\frac{1}{64} & 0 & 0 \\ -\frac{1}{64} & 0 & 0 \end{bmatrix},$$

$$\widetilde{I} = \begin{bmatrix} 0 & 0 & 0 \\ 0 & 0 & 0 \\ 0 & -\frac{1}{16} & 0 \end{bmatrix}, \qquad \widetilde{T} = \begin{bmatrix} 0 & 0 & 0 \\ 0 & 0 & 0 \\ -\frac{1}{128} & 0 & 0 \end{bmatrix}.$$

The subdivision templates for the local averaging rule of this interpolatory $\sqrt{2}$-subdivision scheme are shown in Fig. 33.

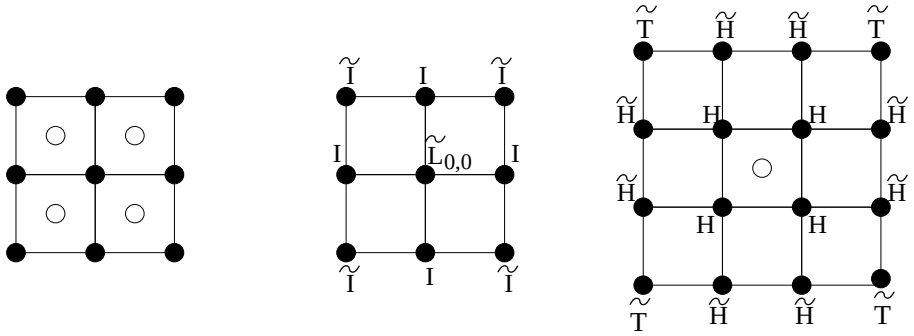

Figure 33: Subdivision templates for the local averaging rule of C^2-quartic spline interpolatory $\sqrt{2}$-subdivision scheme

References

[1] E. Catmull and J. Clark, Recursively generated B-splines surfaces on arbitrary topological meshes, *Comput. Aided Design* **10** (1978), 350–355.

[2] C.K. Chui, *Multivariate Splines*, NSF-CBMS Series #54, SIAM Publ., Philadelphia, 1988.

[3] C.K. Chui and Q.T. Jiang, Surface subdivision schemes generated by refinable bivariate spline function vectors, *Appl. Comput. Harmon. Anal.* **15** (2003), 147–162.

[4] C.K. Chui and Q.T. Jiang, Refinable bivariate C^2-splines for multi-level data representation and surface display, *Math Comp.*, to appear.

[5] C.K. Chui and Q.T. Jiang, Matrix-valued subdivision schemes for generating surfaces with extraordinary vertices, preprint, 2004.

[6] C.K. Chui and Q.T. Jiang, Refinable C^2 quartic and quintic splines for quadrilateral subdivision, preprint, 2004.

[7] C. Conti and G. Zimmermann, Interpolatory rank-1 vector subdivision schemes, *Comput. Aided Geom. Design* **21** (2004), 341-351.

[8] N. Dyn and D. Levin, Analysis of Hermite-interpolatory subdivision schemes, in *Spline functions and the theory of wavelets* (Montreal, PQ, 1996), pp. 105–113, CRM Proc. Lecture Notes, 18, Amer. Math. Soc., Providence, RI, 1999.

[9] N. Dyn, D. Levin, and J.A. Gregory, A butterfly subdivision scheme for surface interpolation with tension control, *ACM Trans. Graphics* **2** (1990), 160–169.

[10] B. Han, Analysis and construction of optimal multivariate biorthogonal wavelets with compact support, *SIAM J. Math. Anal.* **31** (2000), 274–304.

[11] B. Han and R.Q. Jia, Optimal interpolatory subdivision schemes in multidimensional spaces, *SIAM J. Numer. Anal.* **36** (1999), 105–124.

[12] B. Han and R.Q. Jia, Quincunx fundamental refinable functions and quincunx biorthogonal wavelets, *Math. Comp.* **71** (2002), 165–196.

[13] B. Han, T. Yu, and B. Piper, Multivariate refinable Hermite interpolants, *Math Comp.* **73** (2004), 1913–1935.

[14] I.P. Ivrissimtzis, N.A. Dodgson, M.F. Hassan, and M.A. Sabin, On the geometry of recursive subdivision, *Internat. J. Shape Modeling* **8** (2002), 23–42.

[15] I.P. Ivrissimtzis, N.A. Dodgson, and M.A. Sabin, A generative classification of mesh refinement rules with lattice transformations, *Comput. Aided Geom. Design* **21** (2004), 99–109.

[16] I.P. Ivrissimtzis, M.A. Sabin, and N.A. Dodgson, $\sqrt{5}$-subdivision, preprint, 2004.

[17] R.Q. Jia and Q.T. Jiang, Approximation power of refinable vectors of functions, in *Wavelet analysis and applications* (Guangzhou, 1999), 155–178, AMS/IP Stud. Adv. Math., 25, Amer. Math. Soc., Providence, RI, 2002.

[18] R.Q. Jia and Q.T. Jiang, Spectral analysis of transition operators and its applications to smoothness analysis of wavelets, *SIAM J. Matrix Anal. Appl.* **24** (2003), 1071–1109.

[19] Q.T. Jiang, Multivariate matrix refinable functions with arbitrary matrix dilation, *Trans. Amer. Math. Soc.* **351** (1999), 2407–2438.

[20] Q.T. Jiang and P. Oswald, Triangular $\sqrt{3}$-subdivision schemes: the regular case, *J. Comput. Appl. Math.* **156** (2003), 47–75.

[21] Q.T. Jiang, P. Oswald, and S.D. Riemenschneider, $\sqrt{3}$-subdivision schemes: maximal sum rule orders, *Constr. Approx.* **19** (2003), 437–463.

[22] L. Kobbelt, Interpolatory subdivision on open quadrilateral nets with arbitrary topology, *Computer Graphics Forum* **15** (1996), 409–420.

[23] L. Kobbelt, $\sqrt{3}$-subdivision, *SIGGRAPH Computer Graphics Proceedings*, 2000, pp. 103–112.

[24] U. Labsik and G. Greiner, Interpolatory $\sqrt{3}$-subdivision, *Proceedings of Eurographics 2000, Computer Graphics Forum*, 19 (2000), 131–138.

[25] C. Loop, Smooth subdivision surfaces based on triangles, Master's thesis, University of Utah, Department of Mathematics, Salt Lake City, 1987.

[26] P. Oswald, Designing composite triangular subdivision schemes, preprint, 2003.

[27] P. Oswald and P. Schröder, Composite primal/dual $\sqrt{3}$-subdivision schemes, *Comput. Aided Geom. Design* **20** (2003), 135–164.

[28] H. Prautzsch, Analysis of C^k-subdivision surfaces at extraordinary points, preprint 04/98, Fakultät fúr Informatik, Universität Karlsuhe, Germany, 1998.

[29] U. Reif, A unified approach to subdivision algorithms near extraordinary vertices, *Comput. Aided Geom. Design* **21** (1995), 153–174.

[30] S.D. Riemenschneider and Z.W. Shen, Multidimensional interpolatory subdivision schemes, *SIAM J. Numer. Anal.* **34** (1997), 2357–2381.

[31] L. Velho, Quasi 4-8 subdivision, *Comput. Aided Geom. Design* **18** (2001), 345–357.

[32] L. Velho and D. Zorin, 4-8 subdivision, *Comput. Aided Geom. Design* **18** (2001), 397–427.

[33] D.X. Zhou, Multiple refinable Hermite interpolants, *J. Approx. Theory* **102** (2000), 46–71.